SREC-I in macrophages. In an initial attempt to clarify the role of SREC-I in the uptake of modified lipoproteins as well as in the development of atherosclerosis, we generated mice with targeted disruption of the *SREC-I* gene by homologous recombination in embryonic stem cells. To exclude the overwhelming effect of SR-A on the uptake of Ac-LDL, we further generated mice lacking both SR-A and SREC-I (*SR-A*$^{-/-}$;*SREC-I*$^{-/-}$). By comparing the uptake and degradation of Ac-LDL in peritoneal macrophages isolated from these mice, we found that SREC-I plays a significant role in the uptake of Ac-LDL in the setting of SR-A deficiency, especially when stimulated with LPS. From these results, we propose that SREC-I contributes to the development of atherosclerosis in concert with SR-A.

EXPERIMENTAL PROCEDURES

General Methods—Standard molecular biology techniques were used (12). The current experiments were performed in accordance with institutional guidelines for animal experiments at the University of Tokyo and the Jichi Medical School.

SREC-I Antibody Preparation—Two milligrams of the carboxyl-end peptide of mouse SREC-I (amino acid residues 801–820, KEQEEPLYENVVPMSVPPQH) was conjugated with keyhole limpet hemocyanin using the Imject sulfhydryl-reactive antibody production kit (Pierce). The keyhole limpet hemocyanin-peptide was gel-purified and emulsified with an equal volume of complete Freund's adjuvant (Calbiochem). A female Wister rat was immunized with the emulsions. One week after the boost injection, blood was collected, and the antiserum was purified and eluted through an affinity column (Sulfolink coupling gel; Pierce) to which the antigen peptide was coupled.

Mice—SR-A knock-out mice were generated previously (4). ApoE knock-out mice were purchased from the Jackson Laboratory (Bar Harbor, ME) (13). Both mice had been back-crossed to C57BL/6J genetic background and fed a normal chow diet (MF diet from Oriental Yeast Co., Tokyo, Japan) that contained 5.6% (w/w) fat with 0.09% (w/w) cholesterol, and the mice were allowed access to water and food *ad libitum*.

Cells—Thioglycolate-elicited peritoneal macrophages (14) and mouse embryonic fibroblasts (15) were prepared as described previously. Cells were treated with varying concentrations of LPS (*Escherichia coli* O127:B8; Sigma) for 12 h before the experiments.

Northern Blot Analysis—For the SREC-I cDNA probe, two probes were prepared, namely Probe A, a 5′ 2.0-kb fragment spanning the extracellular and intracellular domains, and Probe B, a 0.1-kb fragment consisting of only the transmembrane domain. Poly (A)$^+$ RNA was purified using Oligotex-dT30™, an oligo(dT) latex (Roche Applied Science) from 100–150 μg of total RNA that was extracted by TRIzol reagent (Invitrogen) from either cultured cells or tissues. One to three milligrams of poly(A)$^+$ RNA was subjected to 1% agarose gel electrophoresis in the presence of formalin, transferred to Hybond N (Amersham Biosciences), and hybridized to the ^{32}P-labeled probes for SREC-I and other scavenger receptors as described previously (16).

Western Blot Analysis—Cells were lysed with 0.1% SDS. After centrifugation, 50 μg of the supernatant was subjected to SDS-PAGE and transferred to Hybond ECL™, a nitrocellulose membrane (Amersham Biosciences). After incubation with the anti-SREC-I antibody (1:400 dilution), the membrane was incubated with a goat anti-rat IgG conjugated with horseradish peroxidase (1:2000 dilution; Amersham Biosciences). The secondary antibody was visualized by an enhanced chemiluminescence kit (Amersham Biosciences).

Generation of the SREC-I Knock-out Mice—The *SREC-I* gene was cloned from the 129/Sv mouse genomic library (Clontech) using the mouse cDNA as a probe. A replacement-type targeting vector was constructed so that a 35-bp segment in exon 8, which encodes 3′ two-thirds of the transmembrane domain, was replaced with a polIIneo cassette (Fig. 5*A*). Long arm consists of a 10-kb NotI/KpnI fragment spanning the 5′ untranslated region and exon 8; short arm consists of a 0.9-kb SacI/XbaI fragment within intron 9. These were inserted together into the vector pPolIIshort-neobpA-HSVTK, as described previously (17). After digestion with SalI, the vector was electroporated into JH-1 embryonic stem cells (a generous gift from Dr. Herz at University of Texas Southwestern Medical Center at Dallas, TX). Targeted clones, which had been selected in the presence of G418 and 1-(2-deoxy, 2-fluoro-β-D-arabinofuranosyl)-5 iodouracil, were identified by PCR using the primers 5′-GATTGGGAAGACAATAGCAGGCATGC-3′ and 5′-CAGAGAGTGTCACCACAACAAGAGGA-3′ (Fig. 5*A*). Homologous recombination was verified by Southern blot analysis after digestion with EcoRI using a 0.5-kb SpeI/SmaI fragment, which was downstream of the short arm, as a probe (Fig. 5*A*). Targeted embryonic stem clones were injected into C57BL/6J blastocysts, yielding one line of chimeric mice that transmitted the disrupted allele through the germline.

Generation of the SR-A/SREC-I Double Knock-out Mice—The *SR-A*$^{-/-}$ mice were crossed with the *SREC-I*$^{-/-}$ mice, which were a C57BL/6J × 129/Sv hybrid, to obtain *SR-A*$^{+/-}$;*SREC-I*$^{+/-}$ mice, which were interbred to obtain four types of mice, namely wild-type, *SR-A*$^{+/+}$;*SREC-I*$^{-/-}$, *SR-A*$^{-/-}$;*SREC-I*$^{+/+}$, and *SR-A*$^{-/-}$;*SREC-I*$^{-/-}$ mice. Thus, the genetic background of these mice was 75% C57BL/6J and 25% 129/Sv. Littermates were used for the experiments.

Biochemical Analyses—Blood was collected from the retro-orbital venous plexus after a 12-h fast. Plasma glucose (ANTSENSE II, Bayer Medical, Tokyo, Japan), cholesterol (Determiner TC, Kyowa Medex, Tokyo), and triglycerides (TGLH; Wako Chemicals, Tokyo, Japan) were measured.

Histology—Mice were sacrificed by decapitation. Tissues were excised, fixed in 10% neutral buffered formalin, embedded in paraffin, and stained with hematoxylin-eosin.

Preparation of Lipoproteins—LDL (*d* 1.019–1.063 g/ml) and lipoprotein-deficient serum (*d* >1.21 g/ml) were prepared by stepwise ultracentrifugation from plasma obtained from healthy volunteers. The lipoproteins and lipoprotein-deficient serum were dialyzed against 10 mM sodium phosphate, pH 7.4, 150 mM NaCl, 0.01%(w/v) EDTA, and 0.01% (w/v) NaN_3. LDL was acetylated with acetic anhydrate and radioiodinated by the iodine monochloride method as described (18). Protein concentrations were determined by the BCA protein assay reagent kit (Pierce).

Cellular Uptake and Degradation of ^{125}I-Ac-LDL—Peritoneal macrophages were plated in 12-well plates at a density of 1 × 10^6/well and treated with or without 100 ng/ml of LPS for 12 h. After stringent washing with PBS, the cells were incubated with a medium containing varying concentrations of ^{125}I-Ac-LDL and 5 mg/ml lipoprotein-deficient serum, with or without a 50-fold excess of unlabeled Ac-LDL, for 5 h at 37 °C. The amounts of ^{125}I-Ac-LDL either degraded by or associated with the cells were measured according to a modified method (19) of Goldstein *et al.* (18).

Statistics—The differences of the means were compared by Student's *t* test.

RESULTS

Tissue Distribution of mRNA Expression of SREC-I and -II—We performed Northern blot analyses to examine the expression of SREC-I and II in various organs of a mouse (Fig. 1). SREC-I was expressed in a wide variety of organs, most predominantly in liver, lung, kidney, and heart. On the other hand, the expression of SREC-II was restricted to lung and kidney.

LPS Stimulates the Expression of SREC-I in Peritoneal Macrophages—LPS robustly increased the mRNA expression of both SREC-I and SR-A in macrophages (Fig. 2). The peak of the stimulation was reached by the 12-h time point of the stimulation (Fig. 2*A*), and the maximal responses were obtained at the concentration of 10 ng/ml (Fig. 2*B*). The relative increase in the expression of SREC-I was 4-fold, which was more prominent than that of SR-A (1.8-fold) (Fig. 3). It is of note that the treatment with LPS did not significantly change the expression of MARCO (macrophage receptor with collagenous structure) (20) and SR-BI (21) and that it even decreased the expression of CD36 (22) and FEEL-1 (fasciclin, EGF-like, laminin-type EGF-like, and link domain-containing scavenger receptor-1) (23).

Expression of SREC-I in Aortas—We compared the mRNA expression levels of SREC-I in the atherosclerotic aortas, which were taken from 12-month-old apoE knock-out mice, with normal aortas, mouse embryonic fibroblasts, peritoneal macrophages, kidney, or lung from wild-type mice (Fig. 4). Normal and atherosclerotic aortas expressed 1.7- and 2.1-fold higher levels of SREC-I mRNA than the non-stimulated macrophages, respectively. The expression levels were comparable with those in the kidney, but much lower than those of the LPS-treated macrophages.

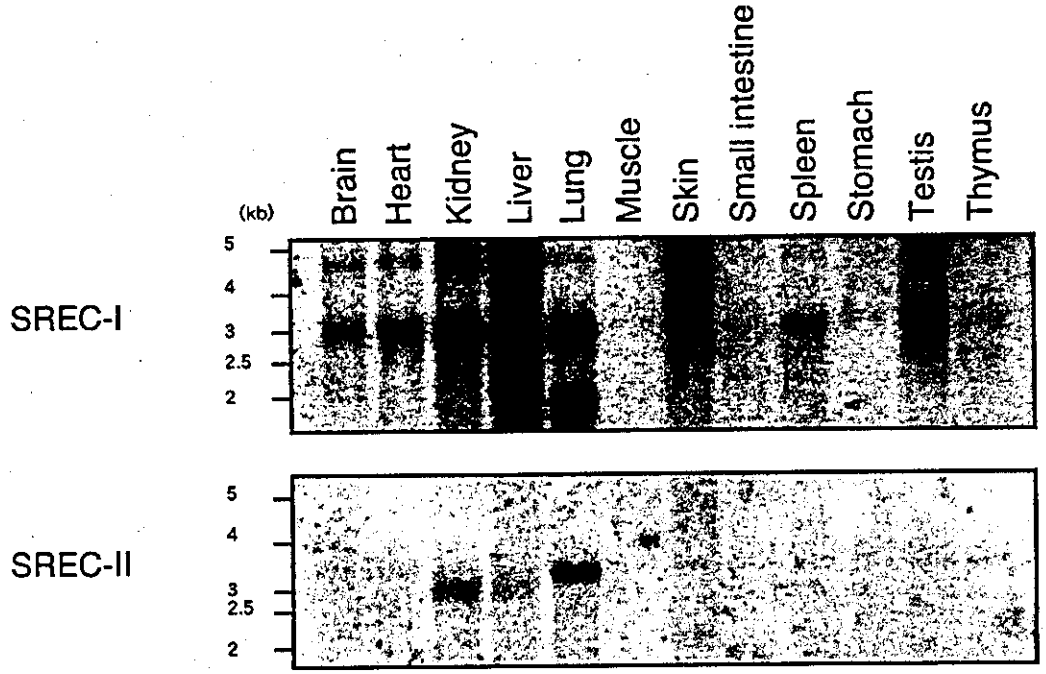

FIG. 1. **Northern blot analysis of SREC-I (*upper panel*) and SREC-II (*lower panel*) in various organs of a mouse.** Two micrograms of poly(A)$^+$ RNA was subjected to Northern blot analysis.

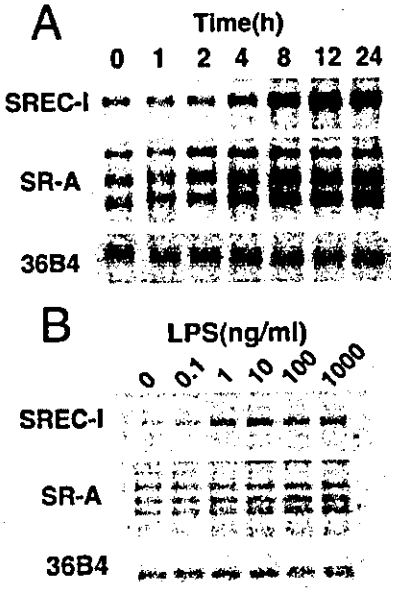

FIG. 2. **Northern blot analysis of SREC-I and SR-A in macrophages treated with LPS.** *A*, thioglycolate-elicited macrophages from C57BL/6 wild-type mice were treated with 100 ng/ml LPS for the indicated times. *B*, cells were treated with the indicated concentrations of LPS for 12 h. Two micrograms of poly(A)$^+$ RNA was subjected to Northern blot analysis. 36B4 was used as a loading control.

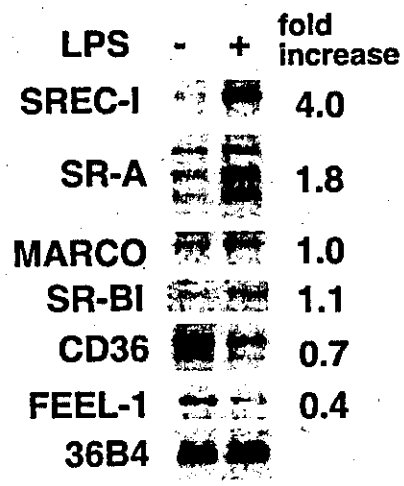

FIG. 3. **Northern blot analysis of scavenger receptors for Ac-LDL in macrophages treated with or without LPS.** Thioglycolate-elicited macrophages from C57BL/6 wild-type mice were treated with (+) or without (−) 100 ng/ml LPS for 12 h. Two micrograms of poly(A)$^+$ RNA was subjected to Northern blot analysis. Probes used were SREC-I, SR-A, MARCO, CD36, SR-BI, and FEEL-1. Signal intensity was corrected against the intensity of 36B4, and the relative signal increase ratio was calculated.

Generation of Mice Lacking the SREC-I and/or SR-A Gene—The intercross of the progeny (*SREC-I*$^{+/-}$) resulted in offspring of both sexes with all three genotypes at the SREC locus with the expected Mendelian ratios (105:191:85 $\chi^2 = 1.06, p > 0.05$) (Fig. 5*B*). Fig. 5*C* shows the results of Northern blot analyses of SREC-I in peritoneal macrophages. When hybridized with Probe A, which contains nearly the whole coding region of the SREC-I cDNA, Northern blot revealed a band with mRNA size of 2.9 kb in wild-type macrophages and a band of 2.4 kb in *SREC-I*$^{-/-}$ macrophages. When hybridized with Probe B, which contains the transmembrane domain, no band was detectable in *SREC-I*$^{-/-}$ macrophages. These results indicate that *SREC-I*$^{-/-}$ mice express a truncated transcript that lacks the transmembrane domain. *SREC-I*$^{-/-}$ mice were fertile and apparently normal. There were no significant differences in the growth curves of wild-type and *SREC-I*$^{-/-}$ mice. As shown in Table I, plasma levels of glucose, cholesterol, and triglycerides were not different between wild-type and *SREC-I*$^{-/-}$ mice. We failed to detect any pathological findings in the brain, lung, heart, liver, kidney, and testis of *SREC-I*$^{-/-}$ mice.

Northern blot analysis of four types of mice confirmed the absence of the expression of SR-A in both *SR-A*$^{-/-}$;*SREC-I*$^{+/+}$ and *SR-A*$^{-/-}$;*SREC-I*$^{-/-}$ mice as well as the expression of the disrupted allele of SREC-I in both *SR-A*$^{+/+}$;*SREC-I*$^{-/-}$ and *SR-A*$^{-/-}$;*SREC-I*$^{-/-}$ mice (Fig. 6*A*). Western blot analysis confirmed the absence of SREC-I protein (~140 and160 kDa) in both *SR-A*$^{+/+}$; *SREC-I*$^{-/-}$ and *SR-A*$^{-/-}$;*SREC-I*$^{-/-}$ mice (Fig. 6*B*).

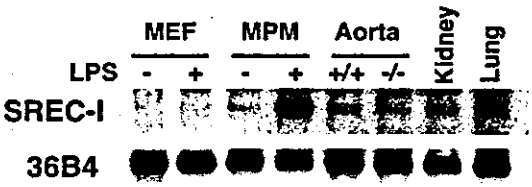

FIG. 4. **Northern blot analysis of SREC-I in normal and atherosclerotic aortas.** RNA were extracted from the following cells or organs: mouse embryonic fibroblasts (*MEF*) treated with (+) or without (−) 100 ng/ml LPS for 12 h; mouse peritoneal macrophages (*MPM*) treated with or without 100 ng/ml LPS for 12 h; kidney; lung; normal aortas from wild-type mice (*Aorta* +/+); and atherosclerotic aortas from apoE−/− mice (*Aorta* −/−). Aortic arches and the thoracic part of descending aortas with rampant visible plaques were excised from five 12-month-old mice. After adipose tissues surrounding the aortas were removed as much as possible, the aortas were used for the preparation of RNA. Three micrograms of poly(A)$^+$ RNA was subjected to Northern blot analysis of SREC-I. 36B4 was used as a loading control.

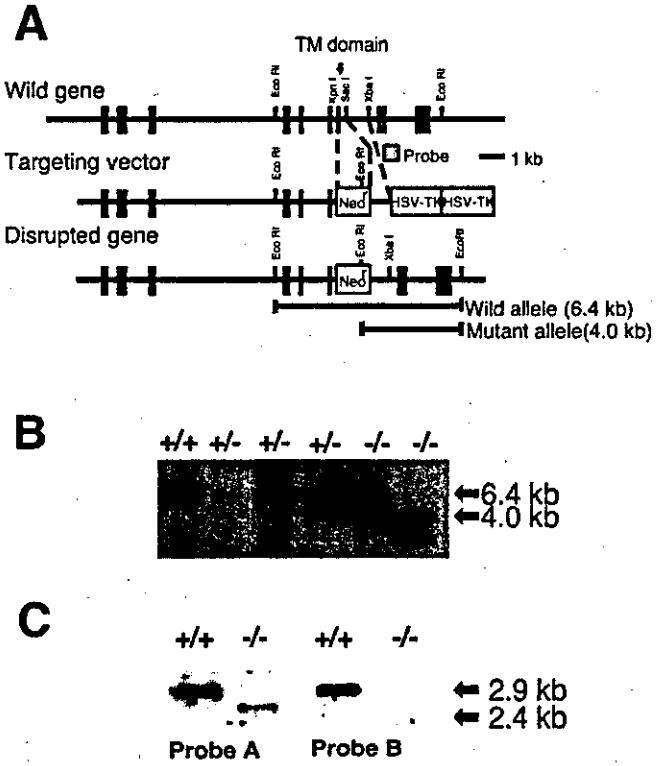

FIG. 5. **Targeted disruption of SREC-I gene.** *A*, map of the SREC-I gene and targeting construct. *Long boxes* represent exons. The exon coding transmembrane domain was replaced with the neomycin resistance gene (*Neo*^{r}) of targeting vector, which has a herpes simplex virus thymidine kinase (*HSV-TK*) cassette for a negative selection downstream of its short arm. A 0.5-kb fragment was used as a probe for Southern blot analysis (*shaded box*). *B*, Southern blot analysis. After digestion with EcoRI, tail DNA was used for Southern blot analysis. The size of the disrupted allele, 4 kb, was smaller than that of wild-type allele (6.4 kb). *C*, mRNA expression of SREC-I in peritoneal macrophage. Two micrograms of poly(A)$^+$ RNA from wild-type (+/+) and *SREC-I*$^{-/-}$ mice (−/−) macrophage was hybridized with two cDNA probes, namely Probe A, a 5′ 2-kb fragment spanning the extracellular and intracellular domains, and Probe B, a 0.1-kb fragment consisting of only the transmembrane domain.

LPS Stimulates Protein Expression of SREC-I—LPS significantly increased the SREC-I protein by ~2-fold in wild-type and *SR-A*$^{-/-}$*;SREC-I*$^{+/+}$ macrophages (Fig. 6*B*).

LPS Increases the Contribution of SREC-I to the Cellular Uptake and Degradation of the ^{125}*I-Ac-LDL*—In non-stimulated conditions (Fig. 7*A*) there was no significant difference in the specific uptake and degradation of ^{125}I-Ac-LDL between wild-type and *SR-A*$^{+/+}$*;SREC-I*$^{-/-}$ macrophages. Based on the values for 20 μg/ml degraded ^{125}I-Ac-LDL, *SR-A*$^{-/-}$*;SREC-I*$^{+/+}$ macrophages degraded significantly smaller amounts of ^{125}I-Ac-LDL (15%) than did wild-type macrophages, supporting the dominant role of SR-A in the uptake and degradation of ^{125}I-Ac-LDL in macrophages. Compared with *SR-A*$^{-/-}$*;SREC-I*$^{+/+}$ macrophages, *SR-A*$^{-/-}$*;SREC-I*$^{-/-}$ macrophages showed a further reduction in the specific uptake (21%) and degradation of ^{125}I-Ac-LDL (31%). Based on the values for 20 μg/ml degraded ^{125}I-Ac-LDL, the contribution of SR-A and SREC-I to the overall degradation of Ac-LDL was calculated to be 85 and 5%, respectively, in the non-stimulated condition.

LPS increased the uptake and degradation of Ac-LDL by 1.8-fold (Fig. 7*B*). In this condition, there was no significant difference in the specific uptake and degradation of ^{125}I-Ac-LDL between wild-type and *SR-A*$^{+/+}$*;SREC-I*$^{-/-}$ macrophages. Based on the values for 20 μg/ml degraded ^{125}I-Ac-LDL,

TABLE I

Plasma levels of glucose, total cholesterol, and triglycerides

After a 12-h fast, blood was collected from the retro-orbital venous plexus of mice aged 8 weeks. Plasma glucose, total cholesterol, and triglycerides were measured. All values are expressed as means ± S.E. No significant deference between wild-type and *SREC-I*$^{-/-}$ mice.

	Wild-type (+/+)	*SREC-I*$^{-/-}$
	mg/dl	
Glucose	61.1 ± 3.2 (n = 31)	63.2 ± 3.2 (n = 31)
Total cholesterol	89.7 ± 5.1 (n = 22)	82.0 ± 3.3 (n = 27)
Triglycerides	89.6 ± 9.4 (n = 22)	97.4 ± 10.3 (n = 27)

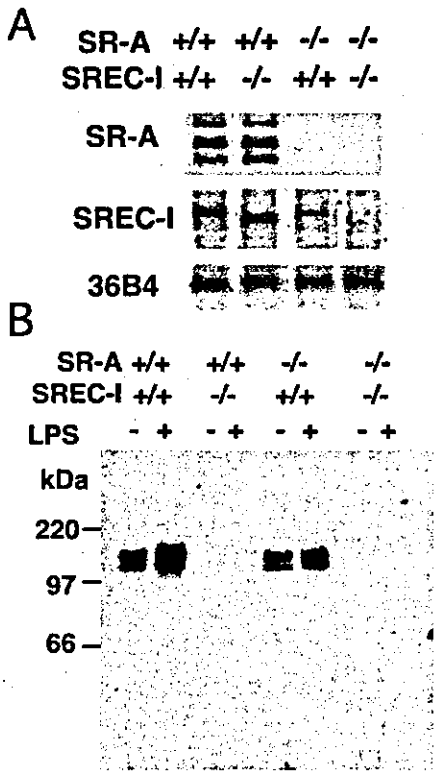

FIG. 6. **Expression of SR-A and SREC-I in macrophages isolated from wild-type, *SR-A*$^{+/+}$*;SREC-I*$^{-/-}$, *SR-A*$^{-/-}$*;SREC-I*$^{+/+}$, and *SR-A*$^{-/-}$*;SREC-I*$^{-/-}$ mice.** Thioglycolate-elicited peritoneal macrophages were prepared from wild-type, *SR-A*$^{+/+}$*;SREC-I*$^{-/-}$, *SR-A*$^{-/-}$*;SREC-I*$^{+/+}$, and *SR-A*$^{-/-}$*;SREC-I*$^{-/-}$ mice. *A*, Northern blot analysis of SR-A and SREC-I. One microgram of poly(A)$^+$ RNA from macrophages was hybridized with SR-A and SREC-I probes (Probe A). *B*, Western blot analysis of SREC-I in macrophages treated with or without LPS. After stimulation with (+) or without (−) 100 ng/ml LPS for 12 h, the cells were lysed with 0.1% SDS, and 50 μg of protein was subjected to SDS-PAGE. Immunoblotting was performed using the rat anti-mouse SREC-I antibody and an enhanced chemiluminescence kit.

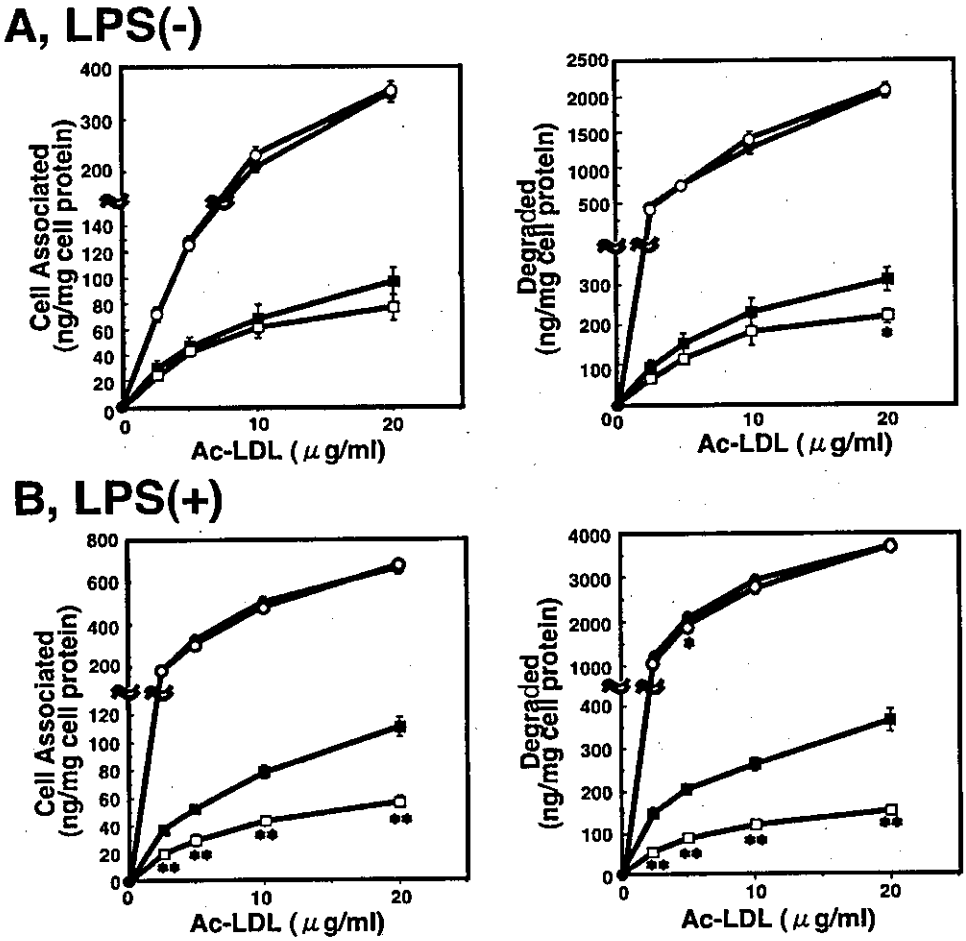

FIG. 7. **Cell association and degradation of ^{125}I-Ac-LDL by peritoneal macrophages isolated from wild-type, *SR-A*$^{+/+}$;*SREC-I*$^{-/-}$, *SR-A*$^{-/-}$;*SREC-I*$^{+/+}$, and *SR-A*$^{-/-}$;*SREC-I*$^{-/-}$ mice.** Thioglycolate-elicited peritoneal macrophages were prepared from four types of mice ($n = 5$), namely wild-type (*solid circle*), *SR-A*$^{+/+}$;*SREC-I*$^{-}$ (*open circle*), *SR-A*$^{-/-}$;*SREC-I*$^{+/+}$ (*solid square*), and *SR-A*$^{-/-}$;*SREC-I*$^{-/-}$ (*open square*). After treatment with (*panel B*) or without (*panel A*) 100 ng/ml LPS for 12 h, the cells were incubated with the indicated concentrations of ^{125}I-Ac-LDL with or without a 50-fold excess of unlabeled Ac-LDL at 37 °C. After 5 h, the amounts of ^{125}I-Ac-LDL associated or degraded were determined. Specific values were calculated by subtracting the nonspecific values from the total values. All values are expressed as means ± S.E. of five mice. *, $p < 0.05$ *versus* *SR-A*$^{-/-}$;*SREC-I*$^{+/+}$ mice; **, $p < 0.01$ *versus* *SR-A*$^{-/-}$; *SREC-I*$^{+/+}$ mice.

SR-A$^{-/-}$;*SREC-I*$^{+/+}$ macrophages degraded significantly smaller amounts of ^{125}I-Ac-LDL (10%) than did wild-type macrophages. Compared with *SR-A*$^{-/-}$;*SREC-I*$^{+/+}$ macrophages, *SR-A*$^{-/-}$;*SREC-I*$^{-/-}$ macrophages showed a further reduction in the specific uptake (49%) and degradation of ^{125}I-Ac-LDL (59%). Based on the values for 20 μg/ml degraded Ac-LDL, the contribution of SR-A and SREC-I to the overall degradation of ^{125}I-Ac-LDL was calculated to be 90 and 6%, respectively. LPS increased the absolute contribution of SR-A and SREC-I by 1.9- and 2.3-fold, respectively. On the other hand, LPS decreased the absolute contribution of other pathways by 31%.

DISCUSSION

In the present study, we have first shown that SREC-I, a novel member of the scavenger receptor family that recognizes modified lipoproteins, is expressed in a wide variety of tissues including macrophages and aortas, implicating its involvement in the development of atherosclerosis. The expression of SREC-I was not significantly different between normal and atherosclerotic aortas, although it was robustly induced by LPS in macrophages, a major cell type that is present in foam cell lesions. To define the precise role of SREC-I, we have generated wild-type, *SR-A*$^{+/+}$;*SREC-I*$^{-/-}$, *SR-A*$^{-/-}$;*SREC-I*$^{+/+}$, and *SR-A*$^{-/-}$;*SREC-I*$^{-/-}$ mice and compared the uptake and degradation of Ac-LDL in macrophages between these mice. Results show that the contribution of SREC-I to the overall uptake and degradation of Ac-LDL was 5% in the non-stimulated condition and 6% in the LPS-stimulated condition. Although the involvement of SREC-I was relatively small compared with that of SR-A, LPS increased the SREC-I mediated degradation by 2.3-fold, which accounted for 60% of the amounts of Ac-LDL degraded by the pathway independent of SR-A.

Because the responses of scavenger receptors to LPS are variable, we did not expect that LPS induced the expression of SREC-I in macrophages. LPS induces SR-A expression in mouse macrophages, which was confirmed in our experiments (Figs. 2 and 3) but not in THP-1 monocyte/macrophages (24) and human monocyte-derived macrophages (25). Because SR-A is able to bind LPS (26), the induction of SR-A by LPS may have a protective role against endotoxemia. This notion is in line with the susceptibility of SR-A knock-out mice to endotoxin shock (4, 27, 28). On the other hand, LPS down-regulates SR-B1 expression (29), which was confirmed in our experiments (Fig. 2).

The mechanism by which LPS induces SREC-I is intriguing. It is well known that LPS modulates gene expression though the activation of NF-κB signaling (30), and some of the effects are mediated by proinflammatory cytokines, whose expression is stimulated by LPS. However, there is no NF-κB binding site in the 5′-flanking region of the human SREC-I gene 1 kb upstream of the transcription initiation site (31). Furthermore,

LPS did not induce SREC-I expression in human umbilical vein endothelial cells, and tumor necrosis factor-α did not have increasing effects on SREC-I expression in mouse macrophages (data not shown). Further studies are warranted to decipher how LPS induces SREC-I expression.

Although SREC-I is expressed in macrophages, particularly when stimulated with LPS, there was no significant difference in the expression levels between normal and atherosclerotic aortas (Fig. 4). This suggests that other cell types such as endothelial cells and smooth muscle cells in the aortas express comparable levels of SREC-I.

SR-A is the major pathway for the uptake and degradation of Ac-LDL, accounting for 80% of the total activity (4, 5). Because other scavengers are expressed in macrophages (Fig. 2) and are able to bind Ac-LDL (2), the question is which scavenger receptor is the second most important in the uptake and degradation of Ac-LDL. Our results have revealed that the role of SREC-I is relatively minor in the non-stimulated macrophages, which is largely consistent with the recent report by Kunjathoor *et al.* (22). According to them, SR-A and CD36 account for 75–90% of the total amounts of chemically modified LDL degraded by macrophages. In SR-A-deficient macrophages stimulated with LPS, however, the absolute contribution of SREC-I was significantly increased by 2.3-fold, accounting for 60% of the SR-A-independent uptake and degradation of Ac-LDL (Fig. 7*B*). The degree of increase in the SREC-I mediated uptake and degradation of Ac-LDL is largely comparable with that in SREC-I protein expression (Fig. 6*B*). It is interesting to note that LPS decreased the absolute contribution of the other endocytic pathway, which is independent of either SR-A or SREC-I, by 31%. This finding is consistent with the Northern blot results that show that LPS did not significantly increase the expression of the other members of scavenger receptor family such as MARCO, SR-BI, CD36, and FEEL-1 (Fig. 3). Thus, SREC-I is the second most important receptor mediating the uptake of Ac-LDL, at least in macrophages stimulated with LPS. Given the activated state of macrophages in rupture-prone unstable plaques (8), particularly in plaques infected with microorganisms such as *Chlamydia*, which is associated with an increased prevalence of coronary events (32), SREC-I may take a significant part in the foam cell formation in these pathological conditions. Other aspects of LPS may be involved in the atherogenesis. For example, Baranova *et al.* (29) and Khovidhunkit *et al.* (33) have recently reported that LPS inhibits high density lipoprotein-mediated cholesterol efflux via down-regulation of the expression of ABCA1 and ABCG1. These observations are consistent not only with the ability of LPS to stimulate lipid accumulation in macrophages *in vitro* (34) but also with the proatherogenic effects of LPS (9) and its cognate receptor, Toll-like receptor 4, *in vivo* (11).

Functions of adhesion molecules have been assigned to both SR-A and SREC-I/II. Chinese hamster ovary cells overexpressing SR-A have an increased ability to adhere to plastic surfaces (35). Likewise, intense aggregation was observed when SREC-I-expressing fibroblast L-cells were mixed with those expressing SREC-II (7). Thus, it is reasonable to speculate that *SREC-I*$^{-/-}$ mice have some phenotypes with regard to cell adhesion. However, there were no obvious abnormalities in the pathologies (data not shown).

The precise roles of scavenger receptors in atherogenesis have been tested only for SR-A and CD36. With regard to SR-A, we (4, 36, 37) and Babaev *et al.* (38) have reported that SR-A deficiency protects against the development of atherosclerosis in either apoE, LDL receptor-deficient, or wild-type mice. de Winther *et al.* (39), however, recently reported apparently opposite results, *i.e.* SR-A deficiency leads to more complex lesions in the APOE3Leiden mice. The same group reported the reduction in atherosclerosis in LDL receptor knock-out mice in which SR-A was overexpressed in a macrophage-specific manner (40). These contradictory results could be attributed to the broad repertoire of functions and the widespread expression of SR-A (41). With regard to CD36, Febbraio *et al.* have reported that CD36 deficiency protects against atherosclerosis in an apoE-deficient background (42). Availability of the *SR-A*$^{-/-}$; *SREC-I*$^{-/-}$ mice should allow us to determine the role of SREC-I in the development of atherosclerosis by crossing with the genetically hyperlipidemic mice, for example. If the hypothesis is correct, SREC-I should be a new target for preventing atherosclerosis.

Acknowledgments—We thank Kimiko Saito, Megumi Herai, Mihoko Kusubae, and Rie Tamura for excellent technical assistance. We also thank Tetsuya Kitamine, Stephane Perrey, Michiyo Amemiya-Kudo, and Takanari Gotoda for helpful comments and discussion.

REFERENCES

1. Brown, M. S., and Goldstein, J. L. (1983) *Annu. Rev. Biochem.* **52,** 223–261
2. Krieger, M. (1997) *Curr. Opin. Lipidol.* **8,** 275–280
3. Kodama, T., Freeman, M., Rohrer, L., Zabrecky, J., Matsudaira, P., and Krieger, M. (1990) *Nature* **343,** 531–535
4. Suzuki, H., Kurihara, Y., Takeya, M., Kamada, N., Kataoka, M., Jishage, K., Ueda, O., Sakaguchi, H., Higashi, T., Suzuki, T., Takashima, Y., Kawabe, Y., Cynshi, O., Wada, Y., Honda, M., Kurihara, H., Aburatani, H., Doi, T., Matsumoto, A., Azuma, S., Noda, T., Toyoda, Y., Itakura, H., Yazaki, Y., Horiuchi, S., Takahashi, K., Kruijt, J. K., Van Berkel, T. J. C., Steinbrecher, U. P., Ishibashi, S., Maeda, N., Gordon, S., and Kodama, T. (1997) *Nature* **386,** 292–296
5. Lougheed, M., Lum, C. M., Ling, W., Suzuki, H., Kodama, T., and Steinbrecher, U. (1997) *J. Biol. Chem.* **272,** 12938–12944
6. Adachi, H., Tsujimoto, M., Arai, H., and Inoue, K. (1997) *J. Biol. Chem.* **272,** 31217–31220
7. Ishii, J., Adachi, H., Aoki, J., Koizumi, H., Tomita, S., Suzuki, T., Tsujimoto, M., Inoue, K., and Arai, H. (2002) *J. Biol. Chem.* **277,** 39696–39702
8. Libby, P. (2002) *Nature* **420,** 868–874
9. Lehr, H. A., Sagban, T. A., Ihling, C., Zahringer, U., Hungerer, K. D., Blumrich, M., Reifenberg, K., and Bhakdi, S. (2001) *Circulation* **104,** 914–920
10. Lynn, W. A., and Cohen, J. (1995) *Clin. Infect. Dis.* **20,** 143–158
11. Vink, A., Schoneveld, A. H., van der Meer, J. J., van Middelaar, B. J., Sluijter, J. P., Smeets, M. B., Quax, P. H., Lim, S. K., Borst, C., Pasterkamp, G., and de Kleijn, D. P. (2002) *Circulation* **106,** 1985–1990
12. Sambrook, J., and Russell, D. W. (2001) *Molecular Cloning: A Laboratory Manual*, Cold Spring Harbor Laboratory Press, Cold Spring Harbor, NY
13. Zhang, S. H., Reddick, R. L., Piedrahita, J. A., and Maeda, N. (1992) *Science* **258,** 468–471
14. Yagyu, H., Kitamine, T., Osuga, J., Tozawa, R., Chen, Z., Kaji, Y., Oka, T., Perrey, S., Tamura, Y., Ohashi, K., Okazaki, H., Yahagi, N., Shionoiri, F., Iizuka, Y., Harada, K., Shimano, H., Yamashita, H., Gotoda, T., Yamada, N., and Ishibashi, S. (2000) *J. Biol. Chem.* **275,** 21324–21330
15. Okazaki, H., Osuga, J., Tamura, Y., Yahagi, N., Tomita, S., Shionoiri, F., Iizuka, Y., Ohashi, K., Harada, K., Kimura, S., Gotoda, T., Shimano, H., Yamada, N., and Ishibashi, S. (2002) *Diabetes* **51,** 3368–3375
16. Tamura, Y., Adachi, H., Osuga, J., Ohashi, K., Yahagi, N., Sekiya, M., Okazaki, H., Tomita, S., Iizuka, Y., Shimano, H., Nagai, R., Kimura, S., Tsujimoto, M., and Ishibashi, S. (2003) *J. Biol. Chem.* **278,** 12613–12617
17. Ishibashi, S., Brown, M. S., Goldstein, J. L., Gerard, R. D., Hammer, R. E., and Herz, J. (1993) *J. Clin. Investig.* **92,** 883–893
18. Goldstein, J. L., Basu, S. K., and Brown, M. S. (1983) *Methods Enzymol.* **98,** 241–260
19. Perrey, S., Ishibashi, S., Kitamine, T., Osuga, J., Yagyu, H., Chen, Z., Shionoiri, F., Iizuka, Y., Yahagi, N., Tamura, Y., Ohashi, K., Harada, K., Gotoda, T., and Yamada, N. (2001) *Atherosclerosis* **154,** 51–60
20. Elomaa, O., Kangas, M., Sahlberg, C., Tuukkanen, J., Sormunen, R., Liakka, A., Thesleff, I., Kraal, G., and Tryggvason, K. (1995) *Cell* **80,** 603–609
21. Acton, S. L., Scherer, P. E., Lodish, H. F., and Krieger, M. (1994) *J. Biol. Chem.* **269,** 21003–21009
22. Kunjathoor, V. V., Febbraio, M., Podrez, E. A., Moore, K. J., Andersson, L., Koehn, S., Rhee, J. S., Silverstein, R., Hoff, H. F., and Freeman, M. W. (2002) *J. Biol. Chem.* **277,** 49982–49988
23. Adachi, H., and Tsujimoto, M. (2002) *J. Biol. Chem.* **277,** 34264–34270
24. Fitzgerald, M. L., Moore, K. J., Freeman, M. W., and Reed, G. L. (2000) *J. Immunol.* **164,** 2692–2700
25. van Lenten, B. J., and Fogelman, A. M. (1992) *J. Immunol.* **148,** 112–116
26. Hampton, R. Y., Golenbock, D. T., Penman, M., Krieger, M., and Raetz, C. R. (1991) *Nature* **352,** 342–344
27. Haworth, R., Platt, N., Keshav, S., Hughes, D., Darley, E., Suzuki, H., Kurihara, Y., Kodama, T., and Gordon, S. (1997) *J. Exp. Med.* **186,** 1431–1439
28. Ishiguro, T., Naito, M., Yamamoto, T., Hasegawa, G., Gejyo, F., Mitsuyama, M., Suzuki, H., and Kodama, T. (2001) *Am. J. Pathol.* **158,** 179–188
29. Baranova, I., Vishnyakova, T., Bocharov, A., Chen, Z., Remaley, A. T., Stonik, J., Eggerman, T. L., and Patterson, A. P. (2002) *Infect Immun.* **70,** 2995–3003
30. Muller, J. M., Ziegler-Heitbrock, H. W., and Baeuerle, P. A. (1993) *Immunobiology* **187,** 233–256

31. Adachi, H., and Tsujimoto, M. (2002) *J. Biol. Chem.* **277,** 24014–24021
32. Becker, A. E., de Boer, O. J., and van Der Wal, A. C. (2001) *Annu. Rev. Med.* **52,** 289–297
33. Khovidhunkit, W., Moser, A. H., Shigenaga, J. K., Grunfeld, C., and Feingold, K. R. (2001) *J. Lipid Res.* **42,** 1636–1644
34. Funk, J. L., Feingold, K. R., Moser, A. H., and Grunfeld, C. (1993) *Atherosclerosis* **98,** 67–82
35. Fraser, I., Hughes, D., and Gordon, S. (1993) *Nature* **364,** 343–346
36. Sakaguchi, H., Takeya, M., Suzuki, H., Hakamata, H., Kodama, T., Horiuchi, S., Gordon, S., van der Laan, L. J., Kraal, G., Ishibashi, S., Kitamura, N., and Takahashi, K. (1998) *Lab. Investig.* **78,** 423–434
37. Kamada, N., Kodama, T., and Suzuki, H. (2001) *J. Atheroscler. Thromb.* **8,** 1–6
38. Babaev, V. R., Gleaves, L. A., Carter, K. J., Suzuki, H., Kodama, T., Fazio, S., and Linton, M. F. (2000) *Arterioscler. Thromb. Vasc. Biol.* **20,** 2593–2599
39. de Winther, M. P., Gijbels, M. J., van Dijk, K. W., van Gorp, P. J., Suzuki, H., Kodama, T., Frants, R. R., Havekes, L. M., and Hofker, M. H. (1999) *Atherosclerosis* **144,** 315–321
40. de Winther, M. P., Gijbels, M. J., van Dijk, K. W., Havekes, L. M., and Hofker, M. H. (2000) *Int. J. Tissue React.* **22,** 85–91
41. Platt, N., and Gordon, S. (2001) *J. Clin. Investig.* **108,** 649–654
42. Febbraio, M., Podrez, E. A., Smith, J. D., Hajjar, D. P., Hazen, S. L., Hoff, H. F., Sharma, K., and Silverstein, R. L. (2000) *J. Clin. Investig.* **105,** 1049–1056

THE JOURNAL OF BIOLOGICAL CHEMISTRY
Vol. 279, No. 38, Issue of September 17, pp. 40084–40090, 2004
Printed in U.S.A.

Type F Scavenger Receptor SREC-I Interacts with Advillin, a Member of the Gelsolin/Villin Family, and Induces Neurite-like Outgrowth*

Received for publication, April 7, 2004, and in revised form, June 30, 2004
Published, JBC Papers in Press, July 9, 2004, DOI 10.1074/jbc.M403844200

Mami Shibata‡§, Junko Ishii‡§¶, Hiroyuki Koizumi‡, Norihito Shibata‡¶, Naoshi Dohmae‖, Koji Takio‖, Hideki Adachi¶, Masafumi Tsujimoto¶, and Hiroyuki Arai‡**

From the ‡Department of Health Chemistry, Graduate School of Pharmaceutical Sciences, University of Tokyo, 7-3-1 Hongo, Bunkyo-ku, Tokyo 113-0033, Japan and the ¶Laboratory of Cellular Biochemistry and ‖Division of Biomolecular Characterization, RIKEN (The Institute of Physical and Chemical Research), 2-1 Wako-shi, Saitama 351-0198, Japan

The scavenger receptor expressed by endothelial cells (SREC) was isolated from a human endothelial cell line and consists of two isoforms named SREC-I and -II. Both isoforms have no significant homology to other types of scavenger receptors. They contain 10 repeats of epidermal growth factor-like cysteine-rich motifs in the extracellular domains and have unusually long C-terminal cytoplasmic domains with Ser/Pro-rich regions. The extracellular domain of SREC-I binds modified low density lipoprotein and mediates a homophilic SREC-I/SREC-I or heterophilic SREC-I/SREC-II trans-interaction. However, the significance of large Ser/Pro-rich cytoplasmic domains of SRECs is not clear. Here, we found that when SREC-I was overexpressed in murine fibroblastic L cells, neurite-like outgrowth was induced, indicating that the receptor can lead to changes in cell morphology. The SREC-I-mediated morphological change required the cytoplasmic domain of the protein, and we identified advillin, a member of the gelsolin/villin family of actin regulatory proteins, as a protein binding to this domain. Reduction of advillin expression in L cells by RNAi led to the absence of the described SREC-I-induced morphological changes, indicating that advillin is a prerequisite for the change. Finally, we demonstrated that SREC-I and advillin were co-expressed and interacted with each other in dorsal root ganglion neurons during embryonic development and that overexpression of both SREC-I and advillin in cultured Neuro-2a cells induced long process formation. These results suggest that the interaction of SREC-I and advillin are involved in the development of dorsal root ganglion neurons by inducing the described morphological changes.

Scavenger receptors are defined by their ability to bind and metabolize modified low density lipoproteins (LDLs),[1] such as acetylated LDL (AcLDL) and oxidized LDL (OxLDL), and have been regarded as relevant in the pathogenesis of atherosclerosis (1, 2). Mammalian cells have several different classes of scavenger receptors, and their relative contributions to lipid metabolism in pathophysiological conditions, such as atherosclerosis, are the subject of intense investigation (2).

Endothelial cells express several distinct scavenger receptors, such as SR-BI (3–5), LOX-1 (6), and FEEl-1/stabilin-1 (7). We cloned a novel scavenger receptor from a DNA library prepared from human umbilical vein endothelial cells employing expression cloning and termed it SREC (scavenger receptor expressed by endothelial cells)-I (8). Subsequently, we also succeeded in cloning a homologous protein, SREC-II, by a data base search (9). These two receptors are now classified as type F scavenger receptors (2, 9).

Both SREC-I and -II have no significant homology to other types of scavenger receptors. They contain 10 repeats of epidermal growth factor-like cysteine-rich motifs in their extracellular domains and unusually long C-terminal cytoplasmic domains with Ser/Pro-rich regions (8, 9). SREC-I mediates the binding and degradation of AcLDL and OxLDL in endothelial cells, whereas SREC-II has little scavenger receptor activity, making it likely that these type F scavenger receptors have biological functions not linked to scavenger receptor activity. We showed previously (9) that SREC-I and -II display respective homophilic interaction through their extracellular domains between separate cells (trans-interaction) and strong SREC-I/SREC-II heterophilic trans-interaction. The homophilic and heterophilic trans-interactions of SREC-I and -II were effectively suppressed by the presence of scavenger receptor ligands, such as AcLDL and OxLDL.

The cytoplasmic domains of SREC-I and -II consisting of ~400 amino acids contain several potential phosphorylation sites for kinases A, C, and G, suggesting that these domains transduce intracellular signals generated by the receptors. SREC-I and -II may transduce different signals because of low sequence similarity and different potential phosphorylation sites. However the biological role of the cytoplasmic domain of SRECs is so far totally unknown.

In this study, we focused on the function of the SREC-I cytoplasmic domain. We previously employed murine L cells to elucidate the receptor/receptor trans-interaction (9), because this cell type is commonly used in experiments demonstrating trans-interaction of various cell adhesion molecules (10–13). In the experiments, we had noticed that prolonged culture of SREC-I-transfected L cells induced striking morphological cell changes. Based on these preliminary observations, we show here that SREC-I, but not SREC-II, induces neurite-like long processes after overexpression in murine fibroblastic L cells and that the cytoplasmic domain of SREC-I is a prerequisite for

* The costs of publication of this article were defrayed in part by the payment of page charges. This article must therefore be hereby marked "*advertisement*" in accordance with 18 U.S.C. Section 1734 solely to indicate this fact.

§ Both authors contributed equally to the results of this work.

** To whom correspondence should be addressed. Tel.: 81-3-5841-4720; Fax: 81-3-3818-3173; E-mail: harai@mol.f.u-tokyo.ac.jp.

[1] The abbreviations used are: LDL, low density lipoprotein; AcLDL, acetylated LDL; OxLDL, oxidized LDL; DRG, dorsal root ganglion; SREC, scavenger receptor expressed by endothelial cells; PBS, phosphate-buffered saline; GST, glutathione *S*-transferase; GFP, green fluorescent protein; DiI, 1,1′-dioctadecyl-3,3,3′,3′-tetramethylindocarbocyanine perchlorate.

this activity. Moreover, we demonstrated that advillin, a member of the gelsolin/villin family of actin regulatory proteins, binds specifically to the cytoplasmic domain of SREC-I and is required for this morphological cell change. The biological implications of this activity are discussed.

EXPERIMENTAL PROCEDURES

Cell Culture—Murine L cells (CCL-1, American Type Culture Collection, Manassas, VA) were maintained in Dulbecco's modified Eagle's medium supplemented with 10% fetal calf serum, 100 units/ml penicillin, 100 mg/ml streptomycin, and 2 mM L-glutamine. Chinese hamster ovary cells were maintained in Ham's F-12 medium supplemented with 50 units/ml penicillin, 50 mg/ml streptomycin, 2 mM L-glutamine, and 10% fetal bovine serum. The murine neuroblastoma line Neuro-2a cells (CCL-131, American Type Culture Collection) were maintained in Dulbecco's modified Eagle's medium supplemented with 10% fetal calf serum, 100 units/ml penicillin, 100 mg/ml streptomycin, and 2 mM L-glutamine.

Plasmid Construction—The EcoRI-XhoI fragment of the mouse cDNA for SREC-I, SREC-I cytoplasmic domain deletion mutant that lacks amino acid residues 451–820 (SREC-I-ΔC370), SREC-II, SR-A, SR-BI, and advillin were subcloned into the mammalian expression vector pcDNA3 (Invitrogen), and expression plasmids were termed pcDNA3-SREC-I, pcDNA3-SREC-I-ΔC370, pcDNA3-SREC-II, pcDNA3-SR-A, pcDNA3-SR-BI, and pcDNA3-advillin, respectively. We noted that a hemagglutinin tag was added at the C terminus of advillin in pcDNA3-Advillin.

Uptake of DiI-AcLDL—L cells (1×10^5 cells/well) in 24-well plates were mock transfected or transfected with either pcDNA3-SREC-I, pcDNA3-SREC-I-ΔC370, pcDNA3-SREC-II, pcDNA3-SR-A, or pcDNA3-SR-BI using LipofectAMINE reagent (Invitrogen) according to the manufacturer's instructions. The cells were incubated for 72 h, incubated again in the presence of 2 μg/ml DiI-AcLDL (Biomedical Technologies Inc.) for 2 h, washed, and then fixed with 3.7% formaldehyde in PBS for 15 min at room temperature. The presence of fluorescent DiI in the fixed cells was determined by visual inspection using fluorescence microscopy.

GST Fusion Proteins—The EcoRI-SalI fragment encoding the first half (C1, amino acid residues 451–643), the central part (C2, amino acid residues 561–752), or the last half (C3, amino acid residues 643–820) of the cytoplasmic domain of mouse SREC-I was subcloned into a multicloning site downstream of the sequence for GST in pGEX-4T-1 (Pharmacia Corporation). This plasmid was transformed into the JM109 strain of *Escherichia coli* and induced with isopropyl-1-thio-β-D-galactopyranoside to produce GST fusion proteins. The bacteria were suspended in PBS, and vigorous sonication was performed before centrifugation at $10,000 \times g$ for 20 min. The resulting supernatants were applied to a glutathione-Sepharose column and then eluted with an elution buffer (50 mM Tris-HCl, pH 9.6, 120 mM NaCl, 10 mM glutathione). Purified GST fusion proteins were dialyzed against PBS containing 2 mM EDTA and 1 mM dithiothreitol.

GST Affinity Chromatography and Peptide Sequence Analysis—L cells (6×10^7 cells) were harvested and homogenized in 1 ml of PBS and then centrifuged at $100,000 \times g$ for 1 h at 4 °C. The resultant supernatant was used as the cytosolic extract. Recombinant GST-C1 or -C2 fusion proteins, bound to the glutathione-Sepharose column, were used to affinity-purify C1- or C2-binding protein(s). L cell cytosolic extracts were loaded onto the GST-C1 or -C2 glutathione-Sepharose columns and then eluted with the elution buffer. The eluted fractions of affinity chromatography were collected, precipitated by 10% trichloroacetic acid, and subjected to SDS-PAGE. A Coomassie Brilliant Blue-stained band of 90 kDa was cut out and digested with *Acromobacter* protease I (API; a gift from Dr. Masaki, Ibaraki University) (14). The resulting peptides were separated by reverse phase high pressure liquid chromatography on tandemly connected DEAE-5PW (1 × 20 mm; Tosoh, Tokyo, Japan) and Capcel Pak C_{18} UG120 (1 × 50 mm; Shiseido, Tokyo, Japan) columns with a 0–80% gradient of acetonitrile in 0.1% trifluoroacetic acid. Isolated peptides were analyzed by automated Edman degradation on an Applied Biosystems protein sequencer model 477A (PerkinElmer Life Sciences) connected on line to a PTH Analyzer model 120A (PerkinElmer Life Sciences) using an in-house-generated gas phase program and were also examined by matrix-assisted laser desorption ionization time-of-flight mass spectrometry with a Reflex MALDI-TOF (Bruker-Franzen Analytik, Bremen, Germany) in linear mode, with 2-mercaptobenzothiazole used as a matrix.

Antibodies—The polyclonal antibodies against SREC-I and advillin were prepared as follows. Peptides corresponding to the C-terminal domain of mouse SREC-I (NH_2-KEQEEPLYENVVPMSVPPQH-COOH) and mouse advillin (NH_2-DGEPKYYPVEVLLKGQNQEL-COOH) were synthesized. The synthesized peptides were conjugated with keyhole limpet hemocyanin using an Imject sulfhydryl-reactive antibody production Kit (Pierce). The keyhole limpet hemocyanin peptides were gel-purified and emulsified with an equal volume of complete Freund's adjuvant (Difco Laboratories, Detroit, MI). Female Wistar rats were immunized with the emulsions. These rat sera were collected and purified using an affinity column (Sulfolink Coupling Gel, Pierce) to which the corresponding antigen peptide was coupled.

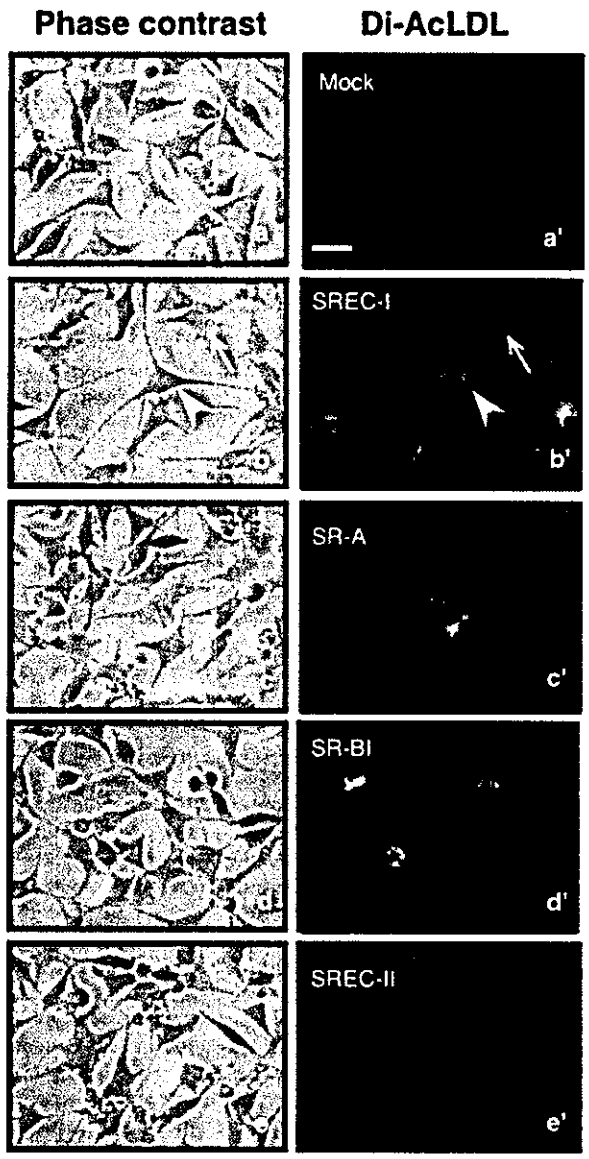

FIG. 1. **SREC-I induces neurite-like long processes in L cells.** Mock-transfected L cells (*a*, *a'*) or L cells transfected with pcDNA3-SREC-I (*b*, *b'*), pcDNA3-SR-A (*c*, *c'*), pcDNA3-SR-BI (*d*, *d'*), or pcDNA3-SREC-II (*e*, *e'*) were incubated with DiI-AcLDL for 2 h. *Left panels*, phase-contrast light micrographs (*a–e*). *Right panels*, fluorescence image (*a'–e'*) of the same fields as in the *left panels*. Note the long processes with the presence of SREC-I (*arrowhead*) and no morphological change with the absence of SREC-I (*arrow*). *Bar*, 10 μm.

Small Interference RNA—The mammalian expression vector pSUPER was used for expression of siRNA in the L cells. Three parts of the gene-specific targeting sequence (19-nucleotide sequences: 1, 5′-AGAAGCCATGCCACTGGTA-3′; 2, 5′-CCGCAGCAGAAAGACGTCG-3′; and 3, 5′-CACAAGGATCAAGGATGAC-3′) from the target transcript separated by a 9-nucleotide noncomplementary spacer (TTCAAGAGA) from the reverse complement of the same 19-nucleotide sequence were inserted in pSUPER. These vectors were referred to as pSUPER-advillin/RNAi-1, -2, and -3, respectively. L cells were transfected with either pSUPER-advillin/RNAi, control vector (pSUPER), pcDNA3-SREC-I plus pSUPER, pcDNA3-SREC-I plus pSUPER-advillin/RNAi, or

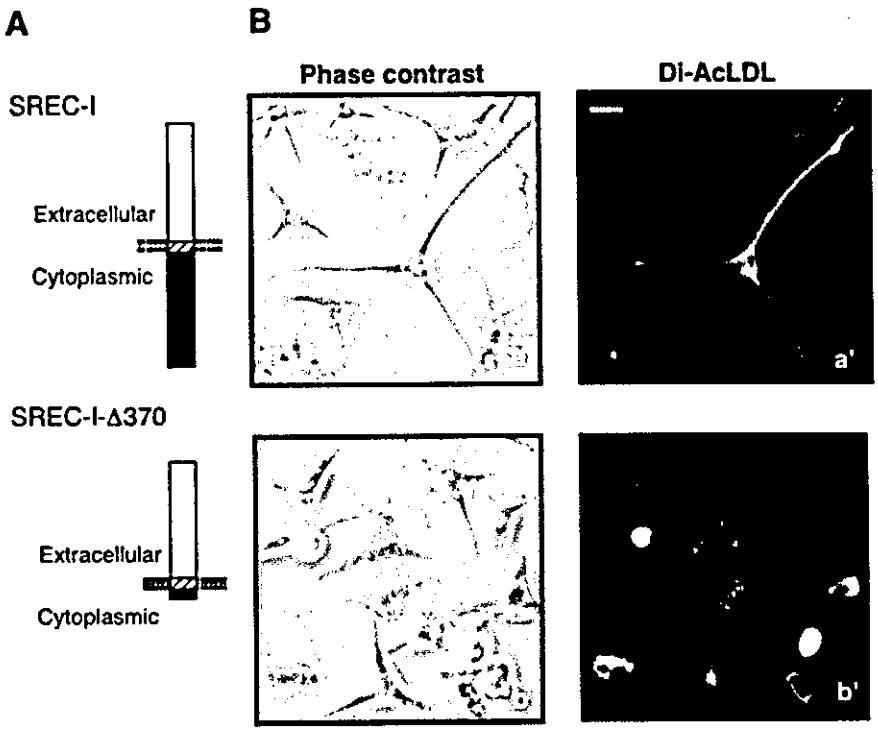

FIG. 2. **SREC-I cytoplasmic domain is required for the induction of morphological change.** *A*, schematic figures of murine SREC-I and SREC-I-ΔC370 showing extracellular, transmembrane, and cytoplasmic sites. *B*, L cells transfected with pcDNA3-SREC-I (*a*, *a'*) or pcDNA3-SREC-I-ΔC370 (*b*, *b'*) were incubated with DiI-AcLDL for 2 h. *Left panels*, phase-contrast light micrographs (*a*, *b*). *Right panels*, fluorescence image (*a'*, *b'*) of the same fields as in the *left panels*. *Bar*, 10 μm.

pcDNA3-GFP plus pSUPER-advillin/RNAi as described above, and the cells were cultured for 72 h. Total cell lysates were prepared in lysis buffer (10 mM Tris-HCl, pH 7.4, 150 mM NaCl, 1% (w/v) Triton X-100, 0.5% (w/v) Nonidet P-40, 1 mM EDTA, protease inhibitor mixture (Sigma), and 1 mM phenylmethylsulfonyl fluoride). The lysates were cleared by centrifugation at 18,600 × *g* for 20 min at 4 °C, were harvested and homogenized in 1 ml of PBS, and then centrifuged at 100,000 × *g* for 1 h at 4 °C. The resultant supernatants were analyzed by Western blotting with anti-advillin or anti-SREC-I antibodies.

Immunofluorescence Microscopy—L cells were transfected with pcDNA3-SREC-I and pSUPER-advillin/RNAi vector or control vector (pSUPER), incubated for 72 h at 37 °C, fixed with 3.7% formaldehyde in PBS for 20 min at room temperature, permeabilized with 0.1% Triton X-100 for 5 min, and then blocked with 3% bovine serum albumin in PBS for 1 h at room temperature. The cells were then incubated with the anti-SREC-I antibody for 2 h at room temperature, washed 4 times with PBS, incubated again with an Alexa Fluor 594 goat anti-rat IgG(H+L) antibody for 1 h at room temperature, washed thoroughly with PBS, embedded, and then visualized using a fluorescent microscope. Neuro-2a cells were transfected with pcDNA3-SREC-I and pcDNA3-advillin, and incubated for 72 h at 37 °C. The cells were then fixed with 3.7% formaldehyde in PBS for 20 min at room temperature, permeabilized with 0.1% Triton X-100 for 5 min, blocked with 3% bovine serum albumin in PBS for 1 h at room temperature, and incubated with the anti-SREC-I antibody and anti-hemagglutinin antibody for 2 h at room temperature. After that, the cells were washed four times with PBS, incubated again with an Alexa Fluor 594 goat anti-rat IgG(H+L) antibody and Alexa Fluor 488 goat anti-mouse IgG(H+L) antibody for 1 h at room temperature, washed thoroughly with PBS, embedded, and then visualized using a fluorescent microscope.

Western Blot Analysis—C57/BL6 mice (adults or 18-day embryos) were perfused with ice-cold SET buffer (0.25 M sucrose, 1 mM EDTA, 10 mM Tris-HCl, pH 7.4) containing protease inhibitor mixture and 1 mM phenylmethylsulfonyl fluoride. Thereafter, the brain, spinal cord, and dorsal root ganglion (DRG) were rapidly excised, as described previously (15). The brain and spinal cord were homogenized in 4 volumes (w/v) of SET buffer and then centrifuged at 1,000 × *g* for 10 min at 4 °C. The resultant supernatants were used as the brain and spinal cord total protein lysates. The DRG was homogenized in SET buffer and then centrifuged at 1,000 × *g* for 10 min at 4 °C. The resultant supernatant was concentrated by 10% trichloroacetic acid precipitation. The resultant pellets were suspended in SET buffer and used as the DRG total protein lysate.

The protein concentrations of samples were determined by BCA assay (Pierce). Each total protein lysate (100 μg/lane) was separated by SDS-PAGE and transferred to nitrocellulose membranes. The membranes were blocked with 5% (w/v) skim milk (Wako, Osaka, Japan) in TTBS buffer (10 mM Tris-HCl, pH 7.4, 150 mM NaCl, 0.05% (w/v) Tween 20) and incubated with anti-advillin or anti-SREC-I antibodies in TTBS. The levels of protein were analyzed with an ECL kit (Amersham Biosciences) according to the manufacturer's instructions.

Immunoprecipitation—DRG extracts were prepared in lysis buffer (10 mM Tris-HCl, pH 7.4, 150 mM NaCl, 1% (w/v) Triton X-100, 0.5% (w/v) Nonidet P-40, 1 mM EDTA, protease inhibitor mixture (Sigma), 1 mM phenylmethylsulfonyl fluoride). The DRG extracts were precleared for 2 h with protein G-agarose beads (Amersham Biosciences) and then incubated overnight with anti-SREC-I antibody at 4 °C. Immunocomplexes were precipitated with protein G-agarose beads for 45 min, washed three times with lysis buffer, and boiled in SDS sample buffer containing 2-mercaptoethanol. The supernatants were subjected to SDS-PAGE and Western blotting.

RESULTS

SREC-I-induced Morphological Change of L Cells—First, L cells were transfected with vectors for various scavenger receptors, and morphological changes were monitored. As shown in Fig. 1, transfection of the expression vector for SREC-I into the cells caused significant morphological changes with generation of neurite-like long processes. On the other hand, no change in cell morphology was observed when other scavenger receptors, such as SR-A, SR-BI, or even SREC-II were overexpressed in these cells. These results suggested that SREC-I is the specific scavenger receptor that can induce neurite-like outgrowth when overexpressed in L cells. When SREC-I was expressed in Chinese hamster ovary cells, no morphological cell change was observed (data not shown).

SREC-I contains a large cytoplasmic domain consisting of ~400 amino acids. To elucidate the role of this cytoplasmic domain, deletion mutants lacking C-terminal fragments of 370 amino acids were created, and their effects on cell shape were examined. We have shown previously (9) that this truncated receptor was expressed in L-cells to a degree similar to the full-length receptor and showed a comparable level of AcLDL uptake activity. In contrast to these findings, the mutant protein did not induce a change in cell morphology (Fig. 2*B*). These results indicated that the cytoplasmic domain is required for the induction of neurite-like outgrowth, and we hypothesized

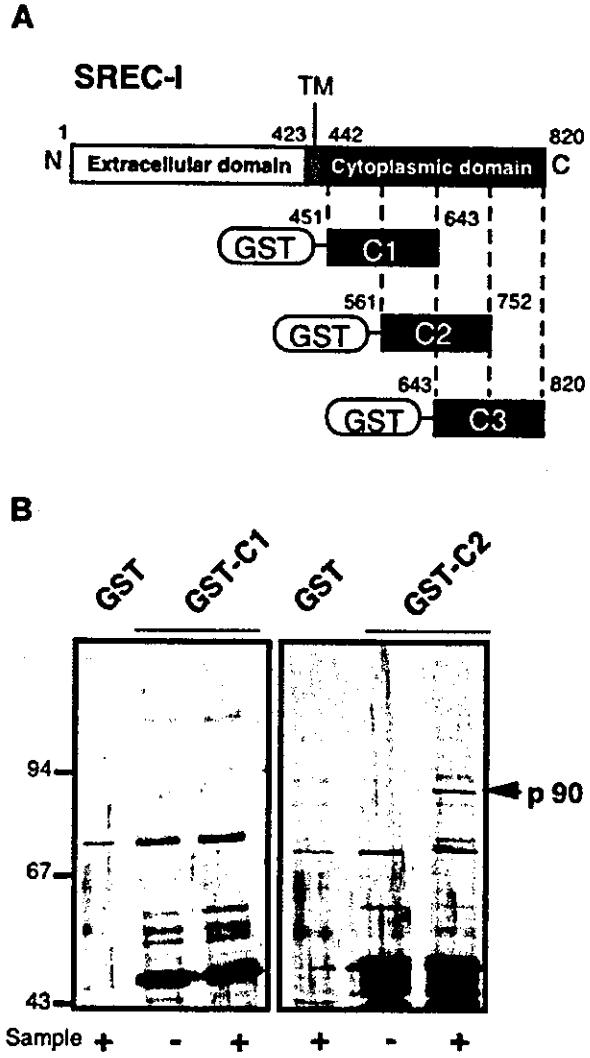

FIG. 3. **Identification of SREC-I cytoplasmic domain-binding proteins.** *A*, the constructs of various deletion mutants of SREC-I fused with GST are shown schematically. *N*, N terminus; *C*, C terminus; *TM*, transmembrane. *Small numbers* refer to amino acid residues. *B*, the L cell cytoplasmic fraction was loaded onto glutathione-Sepharose columns coated with the indicated GST fusion proteins. The bound proteins were eluted by the addition of glutathione. The eluates were subjected to SDS-PAGE followed by silver staining. The *arrow* denotes the position of p90.

that proteins interacting with this domain are required to mediate the effects of this receptor.

Identification of Binding Proteins to the Cytoplasmic Domain of SREC-I—To identify the proteins that bind to the cytoplasmic domain of SREC-I, we prepared several expression vectors for GST-fused C-terminal fragments of the SREC-I protein (Fig. 3*A*, *C1–C3*). Among others, we could successfully express GST-C1 and -C2 fragments in *E. coli* and analyze their binding activities. The cytoplasmic fraction prepared from L cells was loaded onto either a GST-C1 or -C2 affinity column, and the proteins bound to the respective column were co-eluted with GST-fused peptide by the addition of glutathione. As shown in Fig. 3*B*, we could not detect any proteins specifically binding to the C1 fragment. On the other hand, a protein with a molecular mass of ~90 kDa was specifically detected in the glutathione eluate from a GST-C2 column onto which the cytoplasmic fraction of L cells was loaded, although the column loaded with control solution yielded no such protein. These results indicated that the identified 90-kDa protein could bind to the amino acid sequence between residues 643 and 752 of the SREC-I cytoplasmic domain.

The 90-kDa protein was then subjected to amino acid sequencing. Seven peptides derived from the protein were determined, and all were the partial sequences of advillin, an actin regulatory protein belonging to the gelsolin/villin family (16).

Advillin Is Required for SREC-I-mediated Morphological Cell Change—To examine whether advillin is involved in SREC-I-mediated morphological cell change, the RNAi technique was applied (17–20). L cells were treated with several constructs (RNAi-1 to -3; see "Experimental Procedures") of advillin siRNA. First, we confirmed by Western blotting that murine fibroblastic L cells intrinsically expressed advillin (Fig. 4*A*, *lanes 1* of *(a)* and *(b)*, *Advillin*). Moreover, we found that the RNAi-1 vector was most efficient in decreasing the expression of advillin (Fig. 4*A*). Thereafter, L cells were co-transfected with SREC-I and advillin siRNA (RNAi-1) vectors, and morphological cell change was monitored. The expression vector for SREC-I was transfected into the cells, and the expressed protein was analyzed by Western blotting. Two bands with M_r of 141,000 and 147,000 were observed. These two bands were not detected when the green fluorescent protein expression vector was transfected, indicating the heterogeneity of the expressed SREC-I, most probably because of the varying glycosylation of the protein. Co-transfection of RNAi-1 caused a significant decrease in the expression of endogenous advillin without affecting the expression pattern of SREC-I (Fig. 4*B*). As shown in Fig. 4*C*, transfection of the SREC-I vector alone induced neurite-like outgrowth, whereas this phenomenon was impaired significantly by the co-transfection of the RNAi-1 vector. When counting the cells showing long processes, it was apparent that co-transfection of the RNAi-1 vector together with that of SREC-I caused a dramatic decrease in cell number. These results indicate that advillin is required for the SREC-I-mediated induction of neurite-like outgrowth in L cells. It should be noted that unlike in the L cells, advillin was undetectable in Chinese hamster ovary cells in which SREC-I had no apparent ability to induce the described morphological cell change (data not shown).

SREC-I Is Expressed in Peripheral Nerve Neurons—Because it was reported that advillin is expressed in the peripheral nervous system in areas such as the DRG and the superior cervical ganglion and plays a role in the neurite outgrowth of neuronal cells (21), we examined whether SREC-I is also expressed in peripheral nerve neurons. We focused on the embryonic expression of the protein, because it was reported that advillin is expressed in peripheral nerve neurons, especially during embryonic development (16). SREC-I protein was barely detectable in the brain, spinal cord, or DRG of the adult mouse but was clearly detectable in each of these tissues in 18-day embryonic mice (Fig. 5*A*). These results suggested that SREC-I is expressed transiently in the nervous system during fetal development. On the other hand, both in adult and embryonic mice, advillin was detectable in DRG but not in brain or spinal cord.

To determine whether SREC-I interacts with advillin in the DRG of 18-day embryonic mice, we performed immunoprecipitation studies with the anti-SREC-I antibody. Immunoblot analysis revealed that the immunoprecipitates contained advillin in addition to SREC-I (Fig. 5*B*). No anti-SREC-I or anti-advillin signals were detected in the immunoprecipitates treated with normal rabbit serum (data not shown). These results demonstrated that SREC-I interacts with advillin in the DRG of 18-day embryonic mice.

Next, we examined whether the interaction of SREC-I and advillin induces neurite outgrowth in neuronal cells. Because most of the neuronal cell lines intrinsically expressed neither SREC-I nor advillin, we used a murine neuroblastoma cell line,

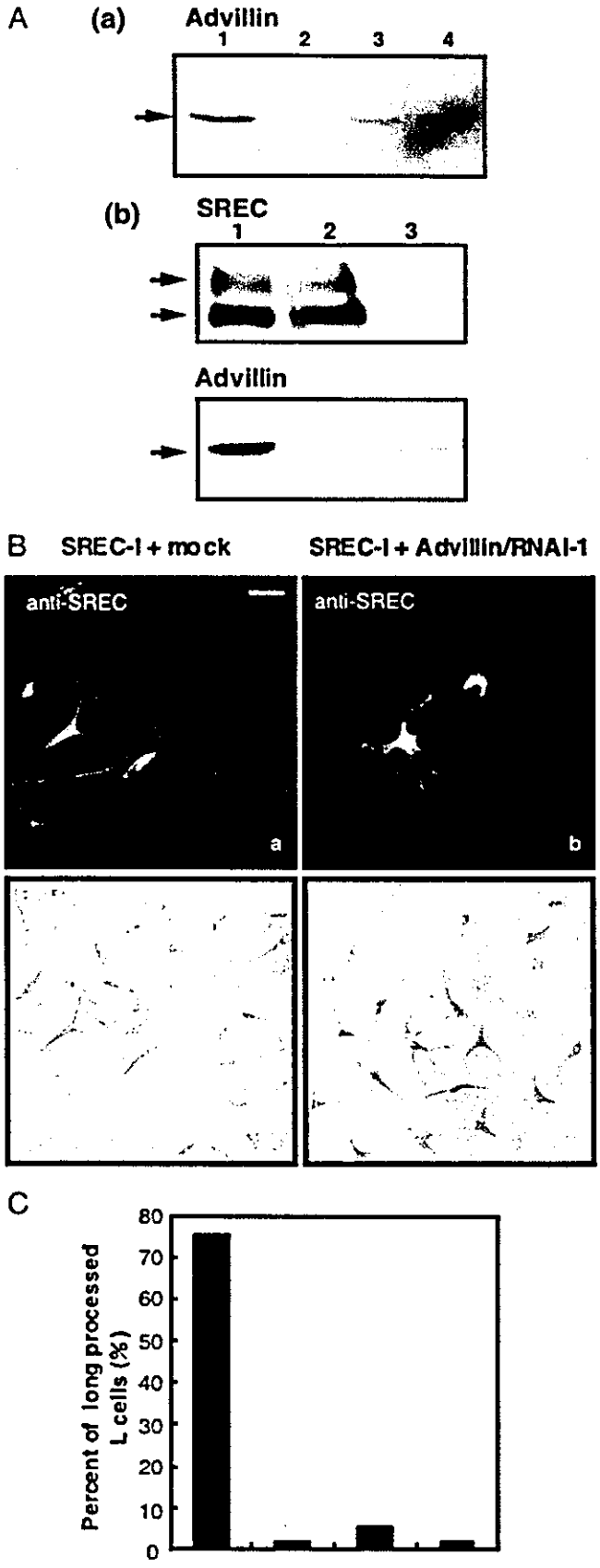

FIG. 4. **Advillin is required for the SREC-I-induced morphological change.** *A*, suppression of advillin expression by pSUPER-advillin/RNAi. (*a*), pSUPER (*lane 1*) or pSUPER-advillin/RNAi-1 to -3 (*lanes 2–4*) were transfected into L cells as described under "Experimental Procedures." Total cell lysates were subjected to SDS-PAGE and immunoblotted to detect advillin proteins. (*b*), pcDNA3-SREC-I and pSUPER (*lane 1*) or pcDNA3-SREC-I and pSUPER-advillin/RNAi-1 (*lane 2*) or pcDNA3-GFP and pSUPER-advillin/RNAi-1 (*lane 3*) were transfected into L cells as described under "Experimental Procedures." Total cell lysates were subjected to SDS-PAGE and immunoblotted to detect SREC-I (*upper panel*) and advillin (*lower panel*) proteins. *B*, L cells transfected with pcDNA3-SREC-I and pSUPER (*left panels*) or pcDNA3-SREC-I and pSUPER-advillin/RNAi-1 (*right panels*) were immunostained with polyclonal antibody against SREC-I. *Upper panels*, fluorescence images. *Lower panels*, phase-contrast light micrographs of the same fields as in the *upper panels*. *Bar*, 10 μm. *C*, percent of >40-μm long processed L cells.

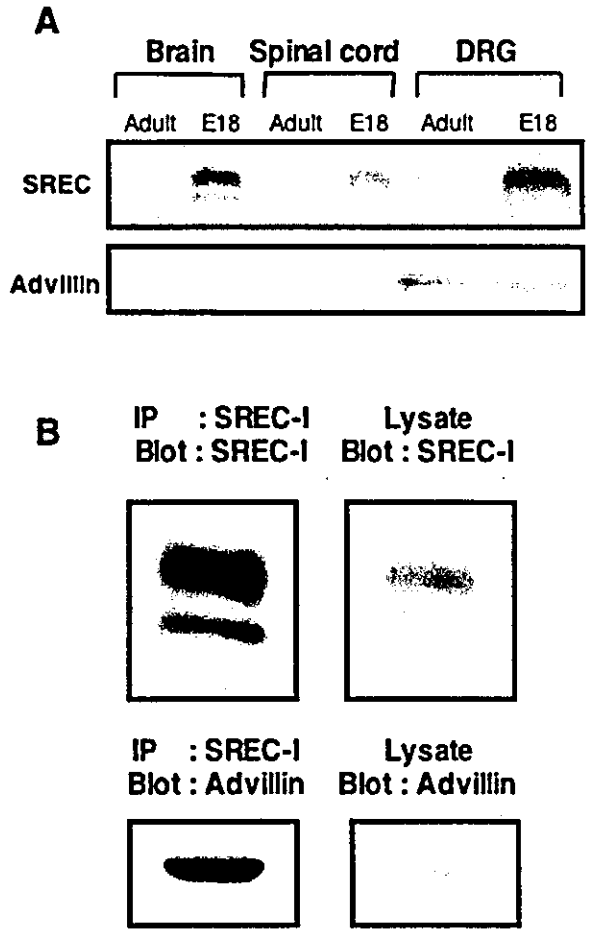

FIG. 5. **Western blot analysis of SREC-I and advillin in murine brain and DRG.** *A*, immunoblot analysis of lysates from mouse brain, spinal cord, and DRG with polyclonal antibody against SREC-I (*upper panel*) and advillin (*lower panel*). Each total protein lysate (100 μg/lane) was separated by SDS-PAGE and subjected to Western blotting. *B*, mouse DRG lysates were immunoprecipitated with polyclonal antibody against SREC-I. Immunoblot analysis of the immunoprecipitates and the lysates with polyclonal antibody against SREC-I (*upper panels*) and advillin (*lower panels*).

Neuro-2a, to perform transfection experiments. The cells were transfected with the SREC-I and/or advillin vectors, and morphological cell change was monitored. As shown in Fig. 6, the cells co-expressing SREC-I and advillin showed neurite outgrowth, whereas the cells expressing either SREC-I or advillin did not show this phenomenon, indicating that the interaction of SREC-I and advillin induces neurite formation in cultured neuronal cells.

DISCUSSION

The present results demonstrate that SREC-I is capable of interacting with advillin (16) through its large Ser/Pro-rich cytoplasmic domain and thereby is capable of inducing neurite-like outgrowth. Members of this actin regulatory protein family are capable of capping and severing actin filaments (16).

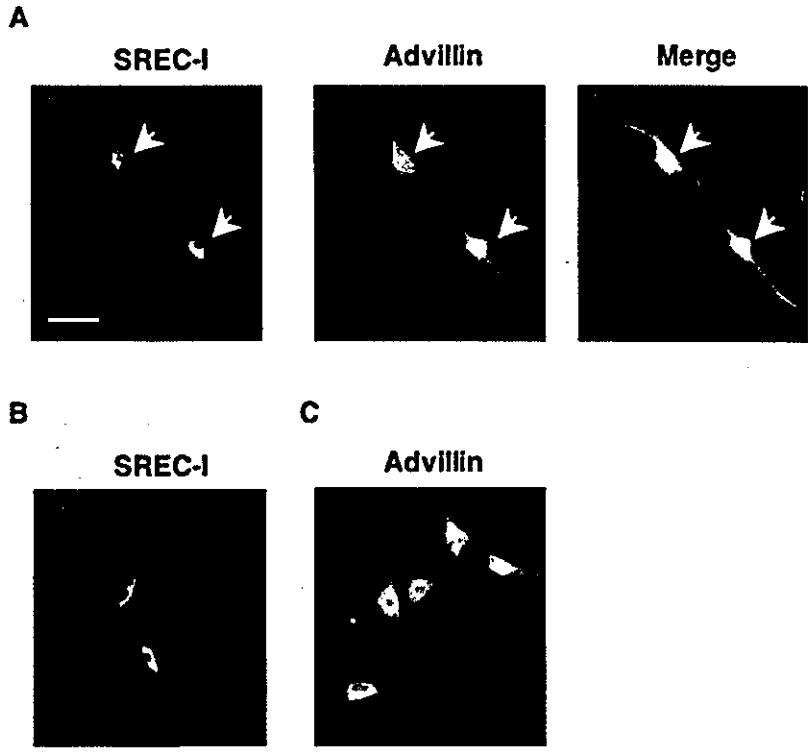

FIG. 6. **Co-expression of SREC-I and advillin induces neurite outgrowth in Neuro-2a cells.** Neuro-2a cells were transfected with pcDNA3-SREC-I and pcDNA3-advillin (*A*), pcDNA3-SREC-I (*B*), or pcDNA3-advillin (*C*). The cells were immunostained with rat polyclonal antibody against SREC-I (*red*) and mouse monoclonal antibody against hemagglutinin-tagged (*green*). Note the long processes with the presence of SREC-I and advillin (*arrowheads*). *Bar*, 20 μm.

Among these proteins, advillin is most closely related to villin in its domain structure, including the C-terminal F-actin-binding headpiece domain (16). Villin is expressed mainly in differentiated epithelial tissues possessing a brush border, such as intestinal villi or proximal renal tubules (22, 23), and most likely plays an important role in the morphogenesis of microvilli (24–26). Advillin, however, is highly expressed in the dorsal root and trigeminal ganglia during embryonic development and only at low levels in adult uterine and intestinal epithelial cells (16). Transfection of the advillin expression vector to primary cultures of rat DRG sensory neurons resulted in increased neurite outgrowth (21), indicating that the protein plays a significant role in the morphogenesis of peripheral neurons through an actin-bundling domain. It is therefore reasonable that the cytoplasmic domain of SREC-I binds to advillin and regulates the intracellular cytoskeletal organization, resulting in the generation of neurite-like long processes.

Unexpectedly, murine fibroblastic L cells were found to intrinsically express advillin (Fig. 4*A*). The parent L strain was derived from normal subcutaneous areolar and adipose tissue of male C3H/An mice according to the CCL-1 catalogue. Intrinsic expression of advillin made it possible to elucidate the function of SREC-I in advillin-mediated morphological changes in L cells. Depletion of endogenous advillin protein in L cells by RNAi inhibited the generation of long processes, indicating that advillin is indispensable for this change. Chinese hamster ovary cells, in which advillin was undetectable, displayed no morphological changes upon SREC-I overexpression. This provides further evidence for the necessity of advillin.

Our results are the first to show that SREC-I is expressed not only in endothelial cells but also in neuronal cells. Furthermore, SREC-I and advillin are co-expressed and interact with each other in DRG neurons, especially during embryonic development. We also demonstrated that overexpression of both SREC-I and advillin in cultured Neuro-2a cells induces the formation of long processes. These results suggest that the interaction of SREC-I and advillin are involved in the development of DRG neurons by inducing the described morphological changes.

SREC-I is characterized by its extremely large cytoplasmic domain. The present data indicate that this domain is a prerequisite for the receptor-mediated morphological change of L cells, which shows that the cytoplasmic domain of SREC-I plays a role in transducing intracellular signals of SREC-I. We showed that advillin binds to the C2 peptide (amino acid residues 562–752) but not to the C1 peptide (amino acid residues 452–643) of the cytoplasmic domain. This suggests that the region within 643–752 is responsible for advillin binding. This region is also rich in Ser and Pro, but it is not similar to the known domains that transduce signals into the cell interior. Interestingly, although ~20% homology was observed in the entire cytoplasmic domains of SREC-I and -II, this region is less homologous (<10%), which can explain why SREC-II exerted no morphogenetic activity on L cells.

It remains unclear how the SREC-I signal is transduced into the cell interior. We have demonstrated previously that SREC-I shows a homophilic trans-interaction between separate cells through its extracellular domain (9). This homophilic trans-interaction of SREC-I may serve as a signal for the induction of neurite-like long processes. However, this may not be the case, because the L cells that display long processes did not necessarily show contact with neighboring SREC-I-expressing L cells (Figs. 1, 2, and 4*B*). Moreover, although homophilic trans-interaction of SREC-I is effectively disrupted by the addition of AcLDL or OxLDL (9), these ligands had little effect on the formation of long processes (data not shown), which supports the idea that trans-interaction of SREC-I between cells is not obligatory for the transduction of the signal into the cells. In our preliminary study, we observed that SREC-I forms an oligomer in the membrane (homophilic *cis*-interaction), possibly a dimer when overexpressed in L cells. The extracellular domain may be indispensable for the oligomerization, because upon co-transfection of native full-length SREC-I and the ΔC370 deletion mutant, which lacks most of the cytoplasmic domain into L cells, both receptors could be co-immunoprecipitated. Interestingly, in most of these cells, long process formation was greatly diminished, indicating that the ΔC370 deletion mutant may function as a dominant

negative effector for SREC-I activity. These observations suggest that close association of the SREC-I cytoplasmic domain themselves may send a signal to L cells that induces the formation of long processes. In *in vivo* situations, some ligands might stimulate SREC-I oligomerization producing a signal in the cells like other growth hormone receptors. SREC-II, which shows a strong heterophilic trans-interaction with SREC-I, is a possible natural ligand for SREC-I. However, in our preliminary experiments, the expression levels of SREC-II in the mouse brain and DRG were very low compared with SREC-I, suggesting that other factor(s) serve as ligands for SREC-I extracellular domains. Further studies are needed to identify the natural ligand in these tissues and to elucidate the mechanism of advillin activation through the SREC-I cytoplasmic domain.

SREC-I was originally identified from a human endothelial cell line (9). Endothelial cells play important roles in vasculogenesis, angiogenesis, and the repair of injuries along the endothelium (27). Under these situations, endothelial cells actively migrate along the substratum in a coordinated and polarized fashion. This process involves extension of filopodia and lamellipodia, both of which have specific actin-based architectures. SREC-I might be involved in the formation and disruption of actin bundles through the gelsolin/villin family in endothelial cells.

REFERENCES

1. Goldstein, J. L., Ho, Y. K., Basu, S. K., and Brown, M. S. (1979) *Proc. Natl. Acad. Sci. U. S. A.* **76,** 333–337
2. Greaves, D. R., Gough, P. J., and Gordon, S. (1998) *Curr. Opin. Lipidol.* **9,** 425–432
3. Acton, S. L., Scherer, P. E., Lodish, H. F., and Krieger, M. (1994) *J. Biol. Chem.* **269,** 21003–21009
4. Yuhanna, I. S., Zhu, Y., Cox, B. E., Hahner, L. D., Osborne-Lawrence, S., Lu, P., Marcel, Y. L., Anderson, R. G., Mendelsohn, M. E., Hobbs, H. H., and Shaul, P. W. (2001) *Nat. Med.* **7,** 853–857
5. Li, X.-A., Titlow, W. B., Jackson, B. A., Giltiay, N. M., Nikolova-Karakashian, M., Uittenbogaard, A., and Smart, E. J. (2002) *J. Biol. Chem.* **277,** 11058–11063
6. Sawamura, T., Kume, N., Aoyama, T., Moriwaki, H., Hoshikawa, H., Aiba, Y., Tanaka, T., Miwa, S., Katsura, Y., Kita, T., and Masaki, T. (1997) *Nature* **386,** 73–77
7. Adachi, H., and Tsujimoto, M. (2002) *J. Biol. Chem.* **277,** 34264–34270
8. Adachi, H., Tsujimoto, M., Arai, H., and Inoue, K. (1997) *J. Biol. Chem.* **272,** 31217–31220
9. Ishii, J., Adachi, H., Aoki, J., Koizumi, H., Tomita, S., Suzuki, T., Tsujimoto, M., Inoue, K., and Arai, H. (2002) *J. Biol. Chem.* **277,** 39696–39702
10. Nagafuchi, A., Shirayoshi, Y., Okazaki, K., Yasuda, K., and Takeichi, M. (1987) *Nature* **329,** 341–343
11. Hatta, K., Nose, A., Nagafuchi, A., and Takeichi, M. (1988) *J. Cell Biol.* **106,** 873–881
12. Aoki, J., Koike, S., Asou, H., Ise, I., Suwa, H., Tanaka, T., Miyasaka, M., and Nomoto, A. (1997) *Exp. Cell Res.* **235,** 374–384
13. Satoh-Horikawa, K., Nakanishi, H., Takahashi, K., Miyahara, M., Nishimura, M., Tachibana, K., Mizoguchi, A., and Takai, Y. (2000) *J. Biol. Chem.* **275,** 10291–10299
14. Masaki, T., Tanabe, M., Nakamura, K., and Soejima, M. (1981) *Biochim. Biophys. Acta* **660,** 44–50
15. Akopian, A. N., and Wood, J. N. (1995) *J. Biol. Chem.* **270,** 21264–21270
16. Marks, P. W., Arai, M., Bandura, J. L., and Kwiatkowski, D. J. (1998) *J. Cell Sci.* **111,** 2129–2136
17. Mise-Omata, S., Montagne, B., Deckert, M., Wienands, J., and Acuto, O. (2003) *Biochem. Biophys. Res. Commun.* **301,** 704–710
18. Hannon, G. J. (2002) *Nature* **418,** 244–251
19. Scherr, M., Morgan, M. A., and Eder, M. (2003) *Curr. Med. Chem.* **10,** 245–256
20. Doi, N., Zenno, S., Ueda, R., Ohki-Hamazaki, H., Ui-Tei, K., and Saigo, K. (2003) *Curr. Biol.* **8,** 41–46
21. Ravenall, S. J., Gavazzi, I., Wood, J. N., and Akopian, A. N. (2002) *Eur. J. Neurosci.* **15,** 281–290
22. Ezell, R., Chafel, M. M., and Matsudaira, P. (1989) *Development (Camb.)* **106,** 407–419
23. Gröne, H., Weber, K., Helmchen, U., and Osborn, M. (1986) *Am. J. Pathol.* **124,** 298–302
24. Franck, Z., Footer, M., and Bretscher, A. (1990) *J. Cell Biol.* **111,** 2475–2485
25. Friederich, E., Huet, C., Arpin, M., and Louvard, D. (1989) *Cell* **59,** 461–475
26. Friederich, E., Vancompernolle, K., Huet, C., Goethals, M., Finidori, J., Vandekerckhove, J., and Louvard, D. (1992) *Cell* **70,** 81–92
27. Kiosses, W. B., Daniels, R. H., Otey, C., Bokoch, G. M., and Schwartz, M. A. (1999) *J. Cell Biol.* **147,** 831–843

別紙４

研究成果の刊行に関する一覧表レイアウト（平成１６年度）

書籍

著者氏名	論文タイトル名	書籍全体の編集者名	書　籍　名	出版社名	出版地	出版年	ページ

雑誌

発表者氏名	論文タイトル名	発表誌名	巻号	ページ	出版年
M. Shibata, J. Ishii, H. Koizumi, N. Shibata, N. Dohmae, K. Takio, H. Adachi, M. Tsujimoto, and H. Arai	Type F scavenger receptor SREC-I interacts with advillin, a member of the gelsolin/villin family, and induces neurite-like outgrowth in mouse fibroblastic L cells	J. Biol. Chem.	279	40084-40090	2004
Tamura Y, Osuga J, Adachi H, Tozawa R, Takanezawa Y, Ohashi K, Yahagi N, Sekiya M, Okazaki H, Tomita S, Iizuka Y, Koizumi H, Inaba T, Yagyu H, Kamada N, Suzuki H, Shimano H, Kadowaki T, Tsujimoto M, Arai H, Yamada N, Ishibashi S	Scavenger receptor expressed by endothelial cells I (SREC-I) mediates the uptake of acetylated low density lipoproteins by macrophages stimulated with lipopolysaccharide.	J. Biol. Chem.	279,	30938-30944	2004)
F. Bonin, S. D. Ryan, L. Migahed, F. Mo, J. Lallier, D. J. Franks, H. Arai, and S. A. L. Bennett	Anti-apoptotic actions of the platelet activating factor acetylhydrolase Ib catalytic subunit	J. Biol. Chem.,	279,	52425-52436	2004

Aβの分解過程に関与する酵素の分子生物学と酵素作用
Angiotensin-converting enzyme (ACE)

内原俊記

Key words: β蛋白分解酵素，ACE inhibitor，AT1 receptor，D/I polymorphism

はじめに

angiotensin-converting enzyme (ACE) は，1,277アミノ酸鎖をもつ糖脂質で，-HEXXH-のZn結合部位を含む2つの活性中心を有する[1]．1個の膜貫通部をカルボキシル末端側にもつtype 1 membrane proteinであるACEは，その名のとおりangiotensin I (Ang I) からC端の2個のアミノ酸を切り離すpeptidyl-dipeptidaseで，Ang IIを産生する酵素として同定された．しかし酵素の基質としてはAng Iのみならず，substance P，cholecystokinin，LH-RHなど多くのペプチドをendopeptidaseとして分解する能力もあり，生体内でもbradykininなどの代謝に関与していることが知られている[2-4]．

renin-angiotensin system (RAS) の代謝に関与する可能性がある酵素はACE以外にも多数あり，活性ペプチドやそのreceptorは中枢神経内にも多種類存在することが知られるようになった(図1)．一方中枢内ではangiotensinogen mRNAの産生などが確認されており，RASを構成する分子は中枢神経系局所でも産生され，生理作用を有していると考えられる．図1に示すRASの酵素反応が神経系のどの細胞のどこで起こっているのかについては不明の部分が多いが，本稿では血圧や体液代謝以外の働きをもつACEの作用[2,3]を，Alzheimer病 (AD) に関連する可能性がある①β蛋白分解作用，②ADのgenetic risk factor，③β蛋白分解以外の作用の観点からまとめる．

1. β蛋白を分解する酵素としてのACE

精製したヒトACEが*in vitro*でAβ1-40をAsp7-Ser8の間で切断し得るとHuらは報告した[5]．こうして切断されたAβはaggregateを作りにくくなり，Aβ線維の形成も遅延する結果，Aβによる細胞障害も*in vitro*では軽減されるという．これらの反応はACE inhibitorの投与により抑制される．しかし正常マウス脳のAβ含有量はACE inhibitorの投与では影響を受けない[6]という報告もあり，ACEが実際に*in vivo*でAβを分解する役割を担っているかどうかは更に検討を要する．

ACEは血管内皮や腎尿細管のbrush borderに局在し，内腔側に活性中心を露出したectoenzymeであり，その酵素作用は主に細胞外で起こるものと想定されている．ヒト脳ではAng IIの免疫活性が血管周囲にあるが，ACE様免疫原性は錐体細胞の細胞体，astrocyteや脈絡膜に限局しており，RASの脳での作用は血管や細胞外に限るものではないことを示唆する[7]．一方Aβについては細胞内のどこで産生されているかは十分に解明されていない部分もあり，ACEの細胞内での局在も明確でないため，ACEが

Toshiki Uchihara: Department of Neuropathology, Tokyo Metropolitan Institute for Neuroscience　東京都神経科学総合研究所神経病理学研究部門

0047-1852/03/¥50/頁/JCLS

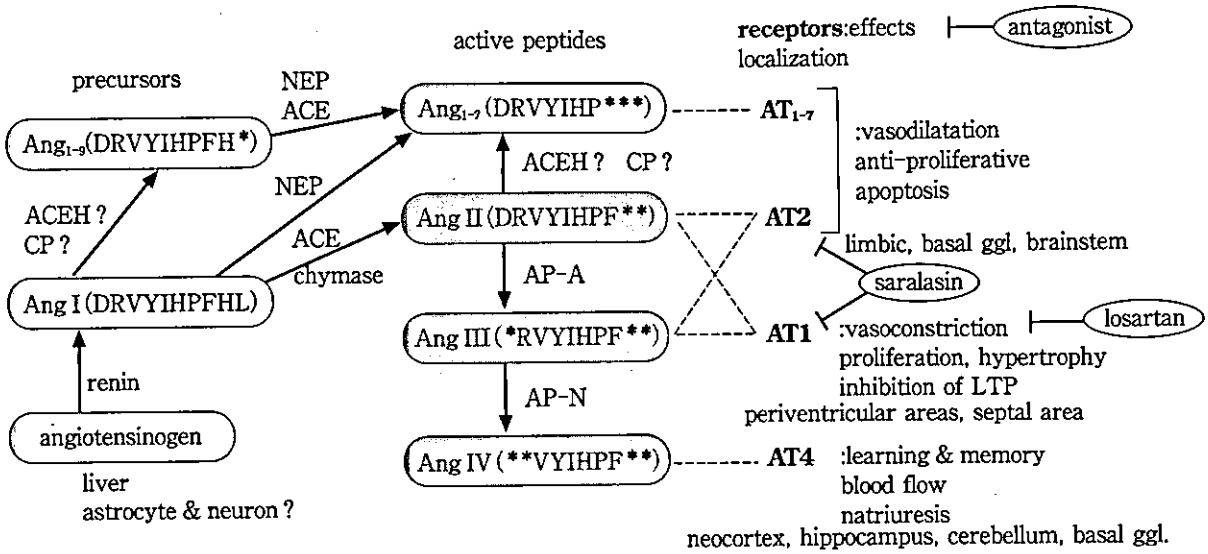

図1 Angiotensinの代謝と機能

各ペプチドのアミノ酸配列と主な変換酵素，receptor，その主な局在と効果を示す．

Ang: angiotensin, *,**,***aminoacid deleted, ACE(H): angiotensin converting enzyme (human homologue), AP: aminopeptidase, CP: carboxypeptidase, NEP: neprilysin (neutral endopeptidase). AT1およびAT2はG-protein coupled receptor, AT4はinsulin-regulated aminopeptidase. AT3はneuroblastoma cell lineで確認されるのみで，生体内での機能は不明．losartanはAT1 antagonist，saralasinはAT1およびAT2 antagonistである．

Aβ分解を触媒するとしてもその作用の場との関係を推測するには情報が十分でない．

AD脳皮質のACE量はその活性からも[8]，免疫染色像からも[7]正常対照に比べて増加している点で，Parkinson病やHuntington病脳とは異なる．またACE inhibitorをligandとしてのbinding siteの総密度も側頭葉で増加しており[9]，特にAT2 receptor siteの上昇が著しい[10]．以上よりRASの活性化がAD脳では起こっているという点で報告の間に矛盾は少ない．逆に脳脊髄液中のACE濃度は正常に比して減少しているとの報告があるが[11]，脳脊髄液に遊離したACEのsoluble formと細胞から離れていないACEではADにおける動態が異なるのかもしれない．

Aβの分解低下はAβの蓄積を招きADの発症を促進するとの仮説があるが[6]，ACEの酵素活性はAD脳で上昇しており，Aβの分解低下を介して沈着を促進するという過程にAD脳で増加しているACEが一次的に関与しているとは解釈しにくい．しかし，ACEを通してAβ分解を促進するADの治療法には意味がないと断定してよいかどうかは一考を要する．

2. ADの危険因子としてのACE遺伝子型

ACE遺伝子座は17q23に位置し，そのintron 16に287 base pair insertがある(I: insertion) alleleとない(D: deletion) alleleに二分される．ACEの発現量はこの遺伝子型により，I/I: 100%とするとI/D: 131%，D/D: 165%と異なる[4]．D/D genotypeはcoronary heart diseaseのrisk factorとされているが，高齢者群ではD/Dを有する割合が有意に多いという報告(**表1-a, b**)もある．D/Dが長寿に関連するかどうかは異論もあるが(**表1-c～e**)，coronary heart diseaseとの関係は一見矛盾するようにみえ，両者を統一的に満たす説明はまだなされていない．

AD(**表1-i～s**)やそれを含む認知障害(**表1-f～h**)に及ぼすこの遺伝子型の影響については多くの研究がある．I alleleがADのriskとなるという報告(**表1-i～l**)は多く，総合的なmeta analysis(**表1-n**)ではそのodds ratioは1.18となるという．逆にD alleleがrisk factorとして有意とする報告(**表1-o, p**)や，遺伝子型による有意差を認めない(**表1-q～u**)との報告もあ

表1　ACE genotypeと年齢，認知機能低下，Alzheimer病との関係

	報告者	数/年齢(平均)歳	数/年齢(平均)歳	人　種	結　果	出典 雑誌名：号：ページ：発行年
		高齢者群	対照群			
a	Schachter	310/100歳以上	164/20-70歳	France	D，DDの頻度が高齢者で高い($p<0.01$)	Nat Genet **6**: 29: 1994
b	Galinsky	270/84歳以上	198/17歳未満	Cambridge	IIの頻度は老人男性のみで低い($p<0.05$)	Atherosclerosis **129**: 177: 1997
c	Agerholm-Larsen	5,343男性/4,807女性	20-90歳	Denmark	年齢層別による遺伝子型の違いはない	Circulation **95**: 2358: 1997
d	Alvarez	117/85歳以上	283/65歳未満	Spain	ns	JNNP **67**: 733: 1999
e	Blanche	560/100歳以上	560(51.2歳)	France	ns	RC Acad Sci **324**: 129: 2001
		認知機能低下群	対照群			
f	Amouyel	228(84歳)CI	255(79歳)	Northern France	D($p<0.012$)，DD(OR=1.63)の頻度はCI群で高い	Neurosci Lett **217**: 203: 1996
g	Bartres-Faz	100(65.8歳)AAMI	124(64.9歳)	Northeastern Iberia	Dの頻度はAAMIで高く60歳代で顕著	Neurosci Lett **290**: 177: 2000
h	Richard	1,168(65歳)でMMSEの経年変化		West France	DD群でMMSE低下が速い例が多い(OR=1.53)	Neurobiol Aging **21**: 75: 2000
		AD群	対照群			
i	Kehoe	542	414	Britain	II+IDの頻度はADで高い(OR=2.22，男性で3.25)	Nat Genet **21**: 71: 1999
j	Alvarez	350	400	Spain	Iの頻度はADで高い(OR=1.28，p=0.03)	JNNP **67**: 733: 1999
k	Yang	188(74.6歳)	227(74.2歳)	Han Chinese	Iの頻度はADで高い(OR=1.45，p=0.01) II+ID/DDのOR=2.09(p=0.0043)，70歳以上で3.37(p=0.0005)	Neurosci Lett **295**: 41: 2000
l	Hu	133(73.1歳)	148(75.5歳)	Japan	II+ID/DDのOR=2.3(p=0.04)	Neurosci Lett **277**: 65: 1999
m	Crawford	171(72.2歳)	175(73.6歳)	Florida	IDの頻度はADで高くID/II+DDのOR=1.67(p=0.018)	Neurosci Lett **280**: 215: 2000
n	Narain	239(81.2歳)	342(82.1歳)	English white	IDの頻度はADで低くID/II+DDのOR=0.64	J Med Genet **37**: 695: 2000
o	Palumbo	140	40	Italy	Dの頻度はADを含む認知障害で高い	Neurosci Lett **267**: 97: 1999
p	Farrer	384	375	Russia+North America	Dの頻度は66-70歳のADで高い(OR=11.2，p=0.02)	Arch Neurol **57**: 210: 2000
q	Chapman	49(74.8歳)	40(72.7歳)	Israel	ns	Stroke **29**: 1401: 1998
r	Scacchi	80(83.5歳)	153(78.3歳)	Italy	ns	Dement Geriatr Cogn Disor **9**: 186: 1998
s	Lendon	119(59歳)ほか95剖検脳	99/30歳以上	Caucasian	ns，Aβやtau沈着量との相関もない	Neurosci Lett **328**: 314: 2002
t	Myllykangas	113ほか121剖検脳	203ほか75剖検脳	Finland	ns	Neurosci Lett **292**: 195: 2000
u	Monastero	149(72.0歳)	149(73.3歳)	Italy	ns	Neurosci Lett **335**: 147: 2002

CI: cognitive impairment，AAMI: age-associated mental impairment，ns: not significant

る．またAD脳のtauやAβの沈着量に対するこの遺伝子型の影響は明らかでないという(表1-s)．ACE遺伝子型とADとの関係に関する結果が報告によって異なるのは，人種差や性差を反映したものとして解釈できるかどうか，今後更に検討を要する．

3. β蛋白分解以外のACEの作用

ACE inhibitorは他の降圧剤に比べて，general well-being，physical symptoms，sexual dysfunctionの改善を自覚的に認める割合が有意に多いという臨床観察があり，RASの中枢への作用が臨床的にも意味があるのではないかと注目されるようになった[12]．

活性をもつangiotensin peptidesは血液脳関門を通過しないとされており，中枢での効果がどのように発現されるかは不明の部分が多い．AngIIを動物の脳室内に投与すると，5HT合成が高まり飲水行動が促進される．またvasopressinergic neuronを刺激しdopamine合成が促進し行動にも変化が現れるという．また*in vivo*や培養細胞ではAngIIはnoradrenaline放出を促進し，放出されたnoradrenalineはAngIIの放出を抑制する形でnegative feedbackをかけている[2-4]．

認知や記憶へのRASの関与についての報告は混乱を極めている．AngIIはヒト脳組織でアセチルコリンの放出を抑制し，海馬やamygdalaではlong term potentiationを抑制する．この抑制はtype 1のangiotensin receptor(AT1)のantagonistであるlosartanで解除される．ACE inhibitorの投与でヒトでは自覚症状の改善がされたり[12]，加齢や薬剤投与によるlearning deficitsがラットで改善することを合わせると，AD脳で報告されたRASの活性亢進は神経伝達物質の放出を修飾することなどを通して認知障害などに関与し得るという推察も成り立つ．しかし脳室にAngIIを投与するとlearningとmemory retensionが改善され，この改善がAT1/AT2 antagonistであるsaralasinで抑制されるという全く逆の結果も報告されており，これらの所見の違いを統一的に説明することは現段階では困難にみえる[2-4]．

4. 今後の展望

最近ACEのヒトhomologue(ACEHまたはACE2)が同定され，ACEとACEHのcatalytic siteの構造は極めて類似していることが明らかにされた．面白いことに，catalytic siteはACEとACEHで類似しているにもかかわらず，ACE inhibitorに対するACEHのaffinityは著しく低いことも示されている[13]．

またangiotensinogenから異なる部分が切り出される結果，AngIIとは異なる生理活性ペプチドも産生される[3]．これらの受容体として，少なくともAT1，AT2，AT4，AT_{1-7}のsubtypeが知られている(図1)．例えばAT4はmemory retentionやretrievalに直接関与しているとの報告があり，AT1 antagonistのlosartanは高血圧患者の認知機能を改善させるという．しかしそれらのligandsや機能について今後更なる検討が必要である[2-4]．

本稿ではACEをはじめとする中枢神経のRASに関するこれまでの研究の一部を概括したが，個々の研究の結論が互いに矛盾する場合もあり，生理機能や病態を分子レベルから包括的に説明するには十分とはいえないのが現状と思われる．しかしACE inhibitorやreceptor antagonistなど強力な薬理作用を有する薬剤が次々と開発されており，治療的介入のための手段は整ってきている．またRASを構成する候補分子は年々数を増しており，例えば受容体特異的な機能を特定できれば，それを制御することを通した特異的な治療法が見いだされる可能性も今後期待される．

文献

1) Natesh R, et al: Crystal structure of the human angiotensin-converting enzyme-lisinopril complex. Nature 421: 551-554, 2003.
2) Wright JW, Harding JW: Important roles for angiotensin III and IV in the brain renin-angiotensin

system. Brain Res Rev **25**: 96–124, 1997.
3) Turner AJ, Hooper NM: The angiotensin-converting enzyme gene family: genomics and pharmacology. Trends Pharmacol Sci **23**: 177–183, 2002.
4) Gard PR: The role of angiotensin II in cognition and behaviour. Eur J Pharmacol **438**: 1–14, 2002.
5) Hu J, et al: Angiotensin-converting enzyme degrades Alzheimer amyloid β-peptide(Aβ); retards Aβ aggregation, deposition, fibril formation and inhibits cytotoxicity. J Biol Chem **276**: 47863–47868, 2001.
6) Iwata N, et al: Identification of the major Aβ1–42-degrading catabolic pathway in brain parenchyma: Suppression leads to biochemical and pathological deposition. Nat Med **6**: 143–150, 2000.
7) Savaskan E, et al: Cortical alterations of angiotensin converting enzyme, angiotensin II and AT1 receptor in Alzheimer's dementia. Neurobiol Aging **22**: 541–546, 2001.
8) Arregui A, et al: Angiotensin converting enzyme in Alzheimer's disease: increased activity in caudate nucleus and cortical areas. J Neurochem **82**: 1490–1492, 1982.
9) Barnes NM, et al: Angiotensin converting enzyme density is increased in temporal cortex from patients with Alzheimer's disease. Eur J Pharmacol **20**: 289–292, 1991.
10) Ge J, Barnes NM: Alterations in angiotensin AT1 and AT2 receptor subtype levels in brain regions from patients with neurodegenerative disorders. Eur J Pharmacol **297**: 299–306, 1996.
11) Zubenko GS, et al: Cerebrospinal fluid levels of angiotensin-converting enzyme, acetylcholinesterase, and dopamine metabolites in dementia associated with Alzheimer's disease and Parkinson's disease: a correlative study. Biol Psychiatry **21**: 1365–1381, 1986.
12) Croog SH, et al: The effects of antihypertensive therapy on the quality of life. N Engl J Med **314**: 1657–1664, 1986.
13) Tipnis SR, et al: A human homolog of angiotensin-converting enzyme. J Biol Chem **275**: 33238–33243, 2000.

Reprinted from JOURNAL OF NEUROLOGY, NEUROSURGERY & PSYCHIATRY, October 2002, Vol 73, No 4, p 450-452

SHORT REPORT

Paradoxical absence of nuclear inclusion in cerebellar Purkinje cells of hereditary ataxias linked to CAG expansion

S Koyano, K Iwabuchi, S Yagishita, Y Kuroiwa, T Uchihara

J Neurol Neurosurg Psychiatry 2002;**73**:450–452

Degeneration of cerebellar cortex is one of the principal features of hereditary ataxias linked to expansion of CAG repeat. In an attempt to clarify possible correlation between neuronal depletion and neuronal intranuclear inclusions, both triggered by the pathological expansion of CAG repeat, cerebellar sections from SCA1, SCA2, SCA3, and DRPLA cases were immunostained with anti-ubiquitin or anti-expanded polyglutamine antibody (1C2) and were screened for the presence of neuronal intranuclear inclusions. Although the degree of cerebellar degeneration varied greatly, cerebellar Purkinje cells were uniformly characterised by the absence of neuronal intranuclear inclusion. Complete absence of neuronal intranuclear inclusion in Purkinje cells is apparently paradoxical and hardly explained if neuronal intranuclear inclusion formation is positively correlated to a mechanism accelerating neuronal death. It may, otherwise, suggest an intrinsic link between neuronal intranuclear inclusion formation and neurodegeneration in opposite directions in human Purkinje cells, more or less affected in these CAG repeat disorders.

At least 10 inherited neurodegenerative diseases, including spinocerebellar ataxias (SCA-1, -2, -3, -6, -7, -12, and -17), Huntington's disease, dentatorubral pallidoluysian atrophy (DRPLA), and spinobulbar muscular atrophy (SBMA) are associated with pathologically expanded CAG repeats in the coding region of the disease gene.[1–3] Because most of them are characterised by the presence of neuronal intranculear inclusions (NIs), which contain the gene product derived from the expanded allele of the responsible gene, formation of NIs induced by expansion of CAG repeat may play a pivotal part in the pathogenesis in common. Although it has been established that an artificial expression of expanded CAG repeat in cultured cells or in transgenic animals induces formation of NIs, it remains to be clarified how NIs are involved in the pathogenesis and neurodegeneration. Accumulating evidence suggests, however, that NI formation is not necessarily correlated with the severity of neuronal degeneration. Discrepancy between neuronal degeneration and formation of NIs has been observed at necopsy in brains with Huntington's disease[4] or with neuronal intranuclear hyaline inclusion disease (NIHID),[5] in mouse transgenic lines carrying mutated ataxin-1,[6] and in some cellular models of polyglutamine diseases.[7] Because it is essential to know how NIs are involved in these degenerative processes, we systematically screened cerebellar cortex in a series of hereditary ataxias in search of ubiquitin or polyglutamine-immunopositive NIs, with special attention to cerebellar Purkinje (Pj) cells, more or less affected in these disorders. A possible role of NI in neurodegeneration and its relation to neuronal death will be discussed.

METHODS

Sections were obtained at postmortem examination from the brains of three SCA1, three SCA2, six SCA3, and five DRPLA patients from unrelated families and three control subjects without neurological and psychiatric disorders. Diagnoses were based on clinical and pathological findings and were confirmed by genomic DNA analysis, as reported previously.[8] Each cerebellum was fixed in 10% formalin for one to three weeks, then cut into 1 cm thick sagittal slices for histopathological and immunohistochemical examination. They were embedded in paraffin wax and four serial slices of 5 μm thick sections were immunostained with an anti-ubiquitin antibody (1:1000, rabbit polyclonal IgG, DAKO, Glostrup, Denmark) or with an anti-polyglutamine antibody, 1C2 (1:9000, mouse monoclonal IgG, Chemicon, Temecula, CA) by using the avidin-biotin-peroxidase complex method (ABC Elite, Vector Burlingane, CA).

RESULTS

Pathological features of these cases were previously summarised.[8] In SCA1 brains, mild to moderate degeneration of the pontocerebellipetal system and of the Pj cells of the cerebellar cortex was found and neuronal loss with grumose degeneration was consistent in the dentate nucleus. SCA2 brains were characterised by severe gliosis involving all three layers of the cerebellar cortex, and loss of Pj cells was uniformly severe in all cases. The dentate nucleus was spared, while some fibrillary gliosis may be seen there in SCA2 brains. In SCA3 and DRPLA brains, the cerebellar cortex was mostly spared, but a slight loss of Pj cells was recognisable. Grumose degeneration was remarkable in the dentate nucleus.

The anti-ubiquitin antibody, at most, lightly immunostained the nucleoplasm and to a lesser extent the cytoplasm of Pj cells in all cases (fig 1 A–D). Ubiquitin-immunopositive NIs were occasionally found in the dentate nucleus of SCA1, SCA3 (fig 1 E) and DRPLA (fig 1 F) cases and rarely in Golgi cells in SCA1 (fig 1 G), SCA2, and DRPLA cases. These NIs were also immunostained with the antibody against expanded polyglutamine (1C2), as shown in fig 1 H (Golgi cell in SCA1). These two antibodies yielded no significant immunolabelling in control cases. Concerning Pj cells, we counted the number of Pj cells in each four serial slices of cerebellum in every case examined in this study (table 1). Approximate mean number of remaining Pj cells per section traversing the dentate nucleus, each including whole sagittal plane of a hemisphere, was about 420 in SCA1, 150 in SCA2, 2320 in SCA3, and 3130 in DRPLA. Neither anti-ubiquitin antibody nor 1C2 identified

Abbreviations: NI, neuronal intranuclear inclusion; Pj, Purkinje; DRPLA, dentatorubal pallidoluysian atrophy; SBMA, spinobulbar muscular atrophy